TLR7/8 activation in neutrophils impairs immune complex phagocytosis through shedding of FcgRIIA

Christian Lood, Sabine Arve, Jeffrey Ledbetter, and Keith B. Elkon

Department of Medicine, Division of Rheumatology, University of Washington, Seattle, WA 98109

Neutrophils play a crucial role in host defense. However, neutrophil activation is also linked to autoimmune diseases such as systemic lupus erythematosus (SLE), where nucleic acid–containing immune complexes (IC) drive inflammation. The role of Toll-like receptor (TLR) signaling in processing of SLE ICs and downstream inflammatory neutrophil effector functions is not known. We observed that TLR7/8 activation leads to a furin-dependent proteolytic cleavage of the N-terminal part of FcgRIIA, shifting neutrophils away from phagocytosis of ICs toward the programmed form of necrosis, NETosis. TLR7/8-activated neutrophils promoted cleavage of FcgRIIA on plasmacytoid dendritic cells and monocytes, resulting in impaired overall clearance of ICs and increased complement C5a generation. Importantly, ex vivo derived activated neutrophils from SLE patients demonstrated a similar cleavage of FcgRIIA that was correlated with markers of disease activity, as well as complement activation. Therapeutic approaches aimed at blocking TLR7/8 activation would be predicted to increase phagocytosis of circulating ICs, while disarming their inflammatory potential.

INTRODUCTION

Neutrophils are the most abundant immune cells in the circulation, participating in host defense through mechanisms including production of reactive oxygen species (ROS), phagocytosis, and formation of neutrophil extracellular traps (NETs), a neutrophil cell death process in which DNA is extruded together with cytoplasmic and granular content to eliminate extracellular pathogens (Nathan, 2006; Pham, 2006; Kaplan and Radic, 2012; Kolaczkowska and Kubes, 2013). Although beneficial from a host–pathogen perspective, exaggerated neutrophil activation has been linked to autoimmunity, in particular the rheumatic disease systemic lupus erythematosus (SLE; Garcia-Romo et al., 2011; Kaplan, 2011; Villanueva et al., 2011; Lood et al., 2016; Lood and Hughes, 2016). In SLE, neutrophil abnormalities were described more than 50 yr ago with the discovery of the lupus erythematosus cell (LE cell), a neutrophil engulfing IgG- and complement-opsonized nuclear debris (Hargraves et al., 1948; Gullstrand et al., 2012). Circulating nucleic acid–containing immune complexes (ICs) participate in SLE pathogenesis through activation of FcgR and complement, and also by engaging intracellular TLR (Lood et al., 2009; Eloranta et al., 2013). We recently demonstrated that RNP containing ICs cause neutrophils to release interferogenic oxidized mitochondrial DNA during NETosis (Lood et al., 2016).

TLR agonists, such as nucleic acids, are important components of pathogens, enabling enhanced phagocytosis by macrophages and DCs (Blander and Medzhitov, 2004; Doyle et al., 2004), as well as inducing cell maturation associated with a shift from phagocytosis to antigen presentation (Watts et al., 2010). Human neutrophils express all TLRs except for TLR3, with TLR8 rather than TLR7 being the most highly expressed single stranded RNA receptor (Hayashi et al., 2003; Berger et al., 2012). Nevertheless, the role of TLR signaling in neutrophil phagocytosis of SLE ICs and their downstream effects has not been extensively investigated. In this study, we reveal a novel mechanism in which TLR7/8 signaling, through shedding of FcgRIIA, shifts neutrophil function from phagocytosis to a programmed necrosis pathway, NETosis. The reverse was also true, namely that phagocytic engagement decreased subsequent NET formation, suggesting neutrophil commitment to either NETosis or phagocytosis dependent on the environmental trigger. Finally, this process is clinically relevant, as SLE patients had evidence for ongoing shedding of FcgRIIA related to neutrophil activation and markers of disease activity.

RESULTS

FcgR and TLR cross talk regulate phagocytosis of RNP-ICs

IC-mediated neutrophil effector functions are thought to play a central role in the lupus pathogenesis (Nathan, 2006; Pham, 2006; Kolaczkowska and Kubes, 2013; Lood et al., 2016). However, mechanisms regulating IC-mediated phagocytosis by neutrophils, and the specific contributions of FcgR and TLR engagement in this process, have not been studied in detail. Using ICs consisting of SmRNP and SLE IgG

Correspondence to Keith B. Elkon: KElkon@medicine.washington.edu; Christian Lood: Loodc@medicine.washington.edu

Abbreviations used: CGD, chronic granulomatous disease; HAGG, heat-aggregated IgG; IC, immune complex; LDG, low-density granulocyte; NET, neutrophil extracellular trap; NETosis, NET formation; ODN, oligodeoxynucleotide; pDC, plasmacytoid DC; ROS, reactive oxygen species; SLE, systemic lupus erythematosus.

The Rockefeller University Press $30.00
J. Exp. Med. 2017 Vol. 214 No. 7 2103–2119
https://doi.org/10.1084/jem.20161512

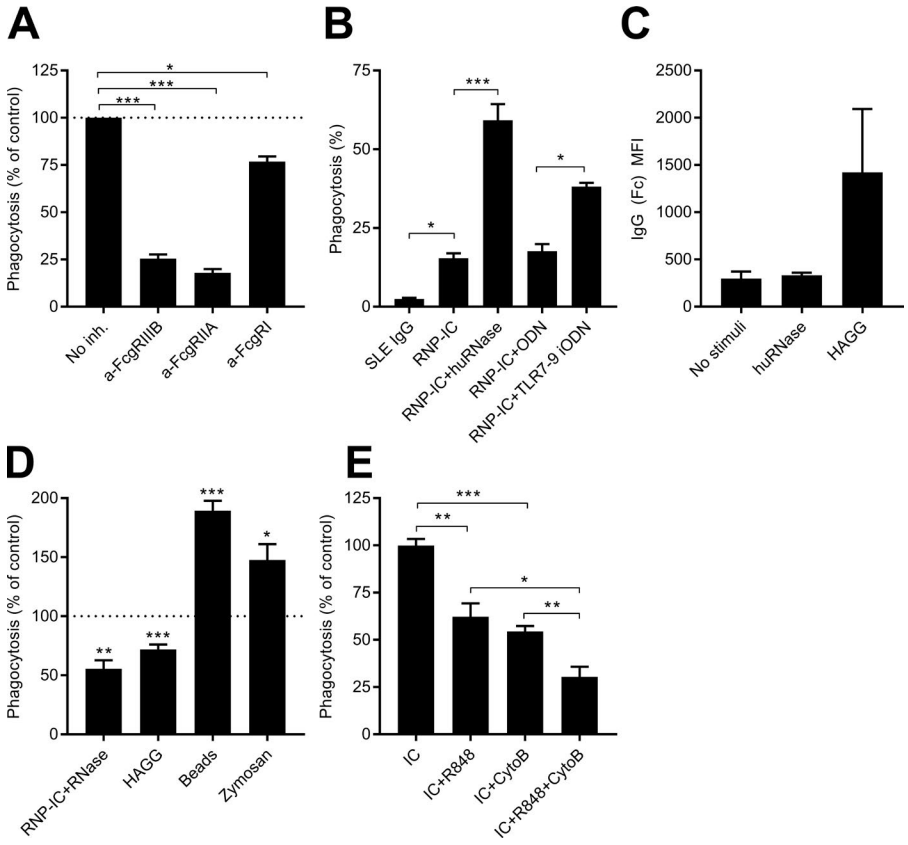

Figure 1. **FcgRIIA and TLR7/8 activation regulates phagocytosis of RNP-ICs.** (A) Neutrophils were incubated with antibodies against FcgRs before stimulation with RNP-ICs. Phagocytosis was quantified by flow cytometry and compared with isotype antibody added (percentage of control). The experiment was repeated three times; combined results are shown and compared using paired Student's *t* test ($P = 0.013$; $P < 0.0001$; $P = 0.0009$ for FcgRI, FcgRIIA, and FcgRIIIB, respectively). (B) TLR7/8 activation was inhibited by RNase or TLR7-9 iODN treatment before incubation of RNP-ICs with neutrophils and phagocytosis analyzed by flow cytometry. The experiment was repeated three times (ODN) or six times (RNase); combined results are compared using paired Student's *t* test ($P = 0.015$; $P = 0.0006$; $P = 0.014$ for SLE IgG, huRNase, and TLR7-9 iODN, respectively). (C) Neutrophils were incubated with human (hu)RNase or HAGG and analyzed for IgG-Fc binding by flow cytometry. The experiment was repeated three times; combined results are shown. (D) Neutrophils were stimulated with R848 before incubation with RNase-treated RNP-ICs, HAGG, beads or zymosan. The results are expressed as phagocytosis as compared with no R848 added (% of control). The experiment was repeated six (zymosan), eight (RNP-IC+RNase), nine (HAGG), or ten (beads) times; combined results are shown and compared using paired *t* test ($P = 0.0005$, $P = 0.0001$, $P < 0.0001$, and $P = 0.017$ for RNP-IC+RNase, HAGG, beads, and zymosan, respectively). (E) Neutrophils, treated with or without R848 followed by cytochalasin B (CytoB; 5 µM), were analyzed for binding and uptake of RNP-ICs by flow cytometry. The experiment was repeated six times; combined results are shown and compared using paired Student's *t* test ($P < 0.0001$ for IC vs. IC+CytoB; $P = 0.0066$ for IC vs. IC+R848; $P = 0.0078$ for IC+CytoB vs. IC+R848+CytoB; and $P = 0.0158$ for IC+R848 vs. IC+R848+CytoB). *, $P < 0.05$; **, $P < 0.01$; ***, $P < 0.001$.

(RNP-ICs), which were previously shown to induce NETosis (Lood et al., 2016) and specific FcgR-blocking monoclonal antibodies, we found that both FcgRIIA and FcgRIIIB were essential for RNP-IC–mediated phagocytosis (Fig. 1 A), whereas FcgRI was dispensable, consistent with the low expression of FcgRI on resting neutrophils. In contrast to studies done in transgenic cell lines and mice with rabbit IgG (Chen et al., 2012), we did not find any evidence of an FcgRIIA-independent role of FcgRIIIB in human neutrophils.

We next asked whether TLR7/8 activation, mediated through the RNA component of the RNP-ICs, influenced the phagocytosis of RNP-ICs by neutrophils. Contrary to expectations, degradation of the TLR ligand by RNase resulted in an increase in the phagocytosis of RNP-ICs by neutrophils (Fig. 1 B). This could not simply be explained by occupancy of the RNase-Fc dimer to FcgRIIA (Fig. 1 C), which is prevented by the P283S mutation, or by changes in the size or character of the RNP-IC, because a similar observation was made when TLR activation was inhibited with a TLR7-9 inhibitory oligodeoxynucleotide (iODN; Fig. 1 B). To determine whether the reciprocal was true, namely that TLR activation could inhibit phagocytosis of ICs, the uptake of RNase-treated RNP-ICs was analyzed in presence of the TLR7/8 agonist, R848. Addition of R848 significantly decreased uptake of ICs, as well as heat-aggregated IgG (HAGG, Fig. 1 D) supporting the hypothesis that TLR activation reduces FcgR-mediated phagocytosis in neutrophils. However, this process was selective; in contrast to ICs, TLR7/8 activation increased uptake of beads and zymosan (Fig. 1 D). Finally, to determine if TLR7/8 activation affected the internalization process and/or the binding ability of the ICs, neutrophils were treated with the cytoskeleton inhibitor Cytochalasin B before adding the ICs, thus blocking uptake, but not binding. As shown in Fig. 1 E, TLR7/8 activation suppressed both IC-mediated binding and subsequent phagocytosis, indicating reduced FcgRIIA function.

TLR7/8 activation induces selective shedding of FcgRIIA

To determine the mechanism for the TLR-induced reduction in RNP-IC phagocytosis, we analyzed the neutrophil surface expression of FcgRs after exposure to TLR ligand. The expression of FcgRIIA was significantly reduced,

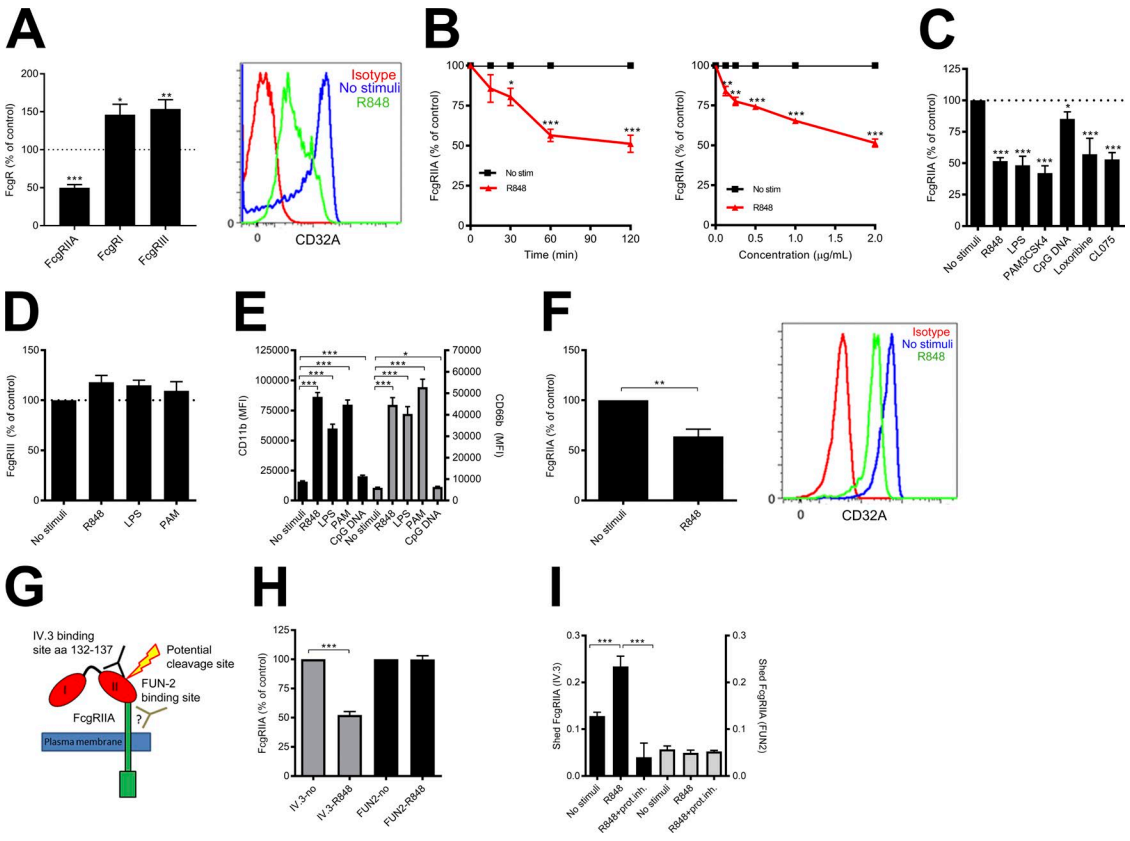

Figure 2. **TLR7/8 activation induces shedding of FcgRIIA.** (A) Neutrophils were activated with R848 and cell surface expression of FcgRs analyzed by flow cytometry. The results are presented as FcgR levels as compared with no R848 added (percentage of control). The experiment was repeated 5 (FcgRI), 7 (FcgRIII), and 25 (FcgRIIA) times; combined results are shown and compared using paired Student's *t* test (FcgRIIA, $P < 0.0001$; FcgRI, $P = 0.027$; FcgRIII, $P = 0.0044$). (B) Neutrophils were activated with the TLR7/8 agonist R848 and analyzed for FcgRIIA at different time-points and concentrations. The experiment was repeated four (concentration) and six (kinetics) times; combined results are shown and compared using paired Student's *t* test (30 min, $P = 0.0158$; 60 min, $P < 0.0001$; 120 min, $P = 0.0003$; 0.125 μg/ml, $P = 0.0071$; 0.25 μg/ml, $P = 0.0058$; 0.5 μg/ml, $P = 0.0008$; 1 μg/ml, $P < 0.0001$; 2 μg/ml, $P < 0.0001$). (C) Neutrophils were activated with TLR ligands (LPS, 1 μg/ml, PAM3CSK4 (5 μg/ml), CpG DNA (2 μg/ml), Loxoribine (0.1 mM), CL075 (2.5 μg/ml), or R848 (2 μg/ml) for 60 min or (D) 4 h and analyzed for (C) FcgRIIA, (D) FcgRIII, or (E) CD11b (black bars) and CD66b (gray bars) cell surface expression by flow cytometry. For C, the experiment was repeated 6 (LPS, $P = 0.0008$), 8 (CpG DNA, $P = 0.035$; Loxoribine, $P < 0.0001$; CL075, $P < 0.0001$), 10 (PAM3CSK4, $P < 0.0001$), and 40 times (R848, $P < 0.0001$); combined results are shown and compared using paired Student's *t* test. For D and E, the experiment was repeated four (D) and eight (E) times; combined results are shown and compared using paired Student's *t* test (CD11b: R848, $P < 0.0001$; LPS, $P = 0.0002$; PAM, $P < 0.0001$; CpG DNA, $P < 0.0001$; CD66b: R848, $P < 0.0001$; LPS, $P < 0.0001$; PAM, $P < 0.0001$; CpG DNA, $P = 0.014$). F) Neutrophils were activated with R848 and FcgRIIA levels analyzed in permeabilized cells by flow cytometry. The experiment was repeated five times and compared using paired Student's *t* test ($P = 0.0075$). (G) Cartoon illustrating the FcgRIIA receptor with the binding site for the IV.3 antibody (aa 132–137), potential cleavage site of FcgRIIA, and likely binding site of FUN2 indicated. (H) FcgRIIA cell surface expression was analyzed by flow cytometry using two antibodies, FUN2 and IV.3, in nonstimulated and R848-stimulated neutrophils. The experiment was repeated six times; combined results are shown and compared using paired Student's *t* test ($P < 0.0001$). (I) Neutrophils were labeled with FITC-conjugated IV.3 anti-FcgRIIA or anti–FUN-2 antibodies and the shed antibody-FcgRIIA complex quantified by fluorimetry after R848 stimulation with or without prior addition of a pan-protease inhibitor. The experiment was repeated 4 (FUN2), 6 (IV.3 R848+prot. inh.), or 14 (IV.3 R848) times; combined results are shown and compared using paired Student's *t* test (IV.3: R848, $P < 0.0001$; R848+prot.inh., $P = 0.0001$). *, $P < 0.05$; **, $P < 0.01$; ***, $P < 0.001$.

whereas surface levels of FcgRIIIB and FcgRI were increased after TLR7/8 stimulation (Fig. 2 A). The decrease in FcgRIIA surface expression was time- and dose-dependent (Fig. 2 B). Loss of FcgRIIA was not specific for TLR7/8 engagement, as neutrophil incubation with either TLR1/2, TLR4, TLR7, or TLR8 selective agonists also reduced neutrophil cell surface levels of FcgRIIA, but not of FcgRIIIB, concomitant with increased expression of CD11b and CD66b (Fig. 2, C–E). Similar results were seen with PMA (unpublished data).

To assess if reduction in FcgRIIA cell surface expression was dependent on proteolytic cleavage or internalization of the receptor, we analyzed total FcgRIIA expression in fixed permeabilized neutrophils. Similar to cell surface staining, R848 reduced the overall FcgRIIA levels in neutrophils (Fig. 2 F). Reduced expression was only seen with one of the antibody

clones tested (IV.3, recognizing amino acid 132–137; Fig. 2 G), but not with the FUN2 clone (Fig. 2 H), indicating that only the most N-terminal part of the FcgRIIA was lost, rather than the full receptor. Furthermore, using cells to which anti-FcgRIIA antibodies had been added (prelabeled), FcgRIIA-IV.3 complexes, but not FcgRIIA–FUN2 complexes, were detected in increased amounts in the cell-free supernatant upon R848 activation compared with nonstimulated cells (Fig. 2 I). Addition of a pan protease inhibitor markedly reduced the overall accumulation of cell-free FcgRIIA–anti-CD32A complexes in the supernatant, indicating that proteolytic cleavage of cell surface FcgRIIA was responsible for reduced FcgRIIA expression after TLR7/8 engagement. The ability of the protease inhibitor to reduce the amount of shed FcgRIIA even further than baseline suggests that basal shedding activity of the neutrophil also occurs in the resting state (Fig. 2 I).

To determine which proteases were involved in the shedding of FcgRIIA, neutrophils were incubated with selective protease inhibitors before the addition of the TLR agonist. As detailed in Fig. 3 A, TLR7/8-mediated shedding of FcgRIIA was dependent on serine proteases, including the pro-protein convertase furin. Although addition of recombinant furin increased cell surface BAFF levels (Fig. 3 B), consistent with current literature (Assi et al., 2007), exogenously added furin did not affect FcgRIIA shedding on neutrophils (Fig. 3 C). Thus, furin most likely did not act directly on FcgRIIA, but on an intracellular process. Although the proteases that cleaves FcgRIIA remains to be identified, we found the neutrophil supernatant to require both a small (<10 kD) heat-sensitive component, as well as a larger (30–100 kD) protein to induce shedding of FcgRIIA (Fig. 3, D and E).

FcgRIIA shedding requires PI3K-dependent generation of reactive oxygen species

As FcgRIIA shedding was associated with the most activated neutrophils (Fig. 4 A), we applied a phosphoproteomic mass spectrometry–based approach to identify proteins and pathways activated by R848 and RNP-ICs that could contribute to shedding of FcgRIIA. Among the identified phosphoproteins, several were involved in cytoskeletal regulation (ADD1, LSP1, VIM, and SYNE1), exocytosis (STXBP5), or MAPK signaling (MAPK14; Fig. 4 B) consistent with the KEGG analysis (Table 1).

Another target of TLR7/8 stimulation was ncf1 (p47 phox; Fig. 4 B, top). Ncf1 was phosphorylated at S345 (Fig. 4, B–D), a known target site involved in activation of the NADPH oxidase complex (Dang et al., 2006). As ROS increases the sensitivity of target proteins for proteolytic degradation (Bota and Davies, 2002) and activates redox-sensitive proteases (Scherz-Shouval et al., 2007), we asked if ROS generation was necessary for shedding of FcgRIIA. Addition of either DPI or apocynin, two well-established inhibitors of NADPH oxidase, completely restored cell surface levels of FcgRIIA (Fig. 4 E). Inhibiting ROS also increased the cell surface expression of FcgRIIB upon TLR7/8 activation, albeit only modestly (unpublished data), suggesting that both FcgRs are negatively regulated through a ROS-dependent mechanism. Consistent with those results, neutrophils from CGD patients, deficient in NADPH oxidase-mediated ROS production, did not show reduced cell surface levels of FcgRIIA upon TLR7/8 engagement (Fig. 4 F), despite CGD neutrophils being able to up-regulate cell surface activation marker, CD66b (Fig. 4 G). TLR1/2 and TLR4-mediated shedding of FcgRIIA was also dependent on NADPH oxidase, suggesting a similar signaling pathway being involved for all TLR agonists (Fig. 4 H). To determine if TLR7/8-mediated ROS was generated intracellularly, or released extracellularly by plasma membrane–located NADPH oxidase complexes, we analyzed the cellular localization of ROS using cell-impermeable ROS dyes and flow cytometry. Both R848 and RNP-ICs induced intracellular generation of ROS, but no detectable extracellular ROS, whereas PMA induced both intracellular and extracellular ROS generation (Fig. 4 I), suggesting formation of endosomal, but not cell surface, NADPH oxidase complexes after stimulation with RNP-ICs and R848.

We next asked which pathways were acting upstream of NADPH oxidase to induce FcgRIIA shedding. Several regulators of NADPH oxidase have been demonstrated, among which PI3K is central (Hawkins et al., 2007), and known to be essential in IC-mediated neutrophil activation (Kulkarni et al., 2011). Neutrophil TLR7/8 ligation induced increased levels of phosphorylated Akt and S6 as determined by flow cytometry (Fig. 4 J), and S6 was one of the most phosphorylated proteins as determined by phosphoproteomics (Fig. 4 B, bottom arrow), strongly suggesting PI3K activation upon TLR7/8 activation. To confirm the role for PI3K in TLR-mediated activation of ROS and subsequent shedding of FcgRIIA, neutrophils were incubated with the PI3K inhibitor LY294002 before addition of TLR agonist. Blocking PI3K signaling abrogated TLR-mediated ROS generation (Fig. 4 K), phosphorylation of ncf1 at S345 (Fig. 4 D), and shedding of FcgRIIA (Fig. 4 L). Also, heat-aggregated IgG (HAGG) cross-linking of FcgRIIA activated neutrophils to induce shedding of FcgRIIA in a PI3K-dependent manner, albeit to a lesser extent than TLR activation (Fig. 4, M–O). Collectively, these data demonstrate that PI3K-driven ROS production via NADPH oxidase is necessary for TLR-7/8-mediated shedding of FcgRIIA.

Table 1. **KEGG pathway analysis upon TLR7/8 activation**

KEGG pathway	P-value
FcgR-mediated phagocytosis	0.00014
Regulation of actin cytoskeleton	0.0035
Endocytosis	0.032
MAPK signaling pathway	0.043

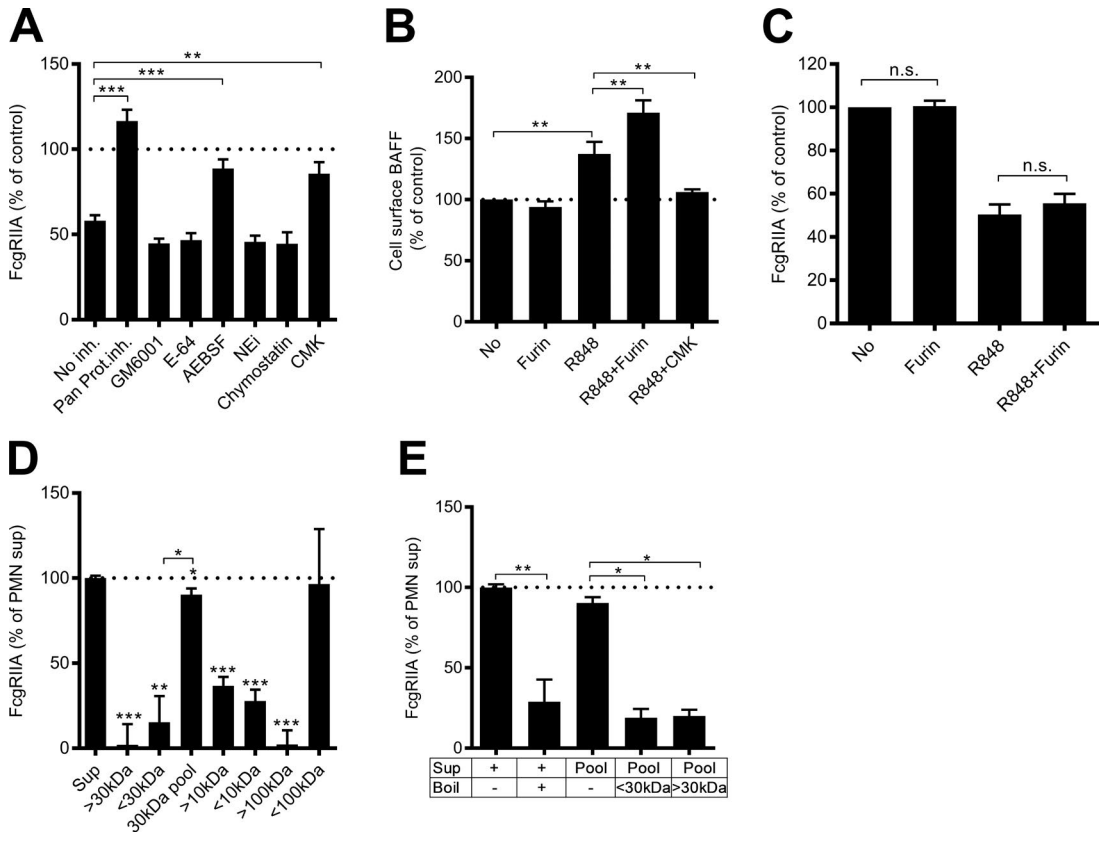

Figure 3. **FcgRIIA shedding requires serine proteases.** (A) Cell surface levels of FcgRIIA (IV.3) was analyzed by flow cytometry upon R848 activation in the presence of a pan protease inhibitor or inhibitors of matrix metalloproteases (GM6001, 10 µM), cysteine proteases (E-64, 1 µM), serine proteases (AEBSF, 100 µM), neutrophil elastase (Elastase inhibitor IV, 25 µM), cathepsin G (chymostatin, 10 µg/ml), or furin (chloromethylketone (CMK, 25 µM). The experiment was repeated three (E-64), four (Pan Prot.inh., $P < 0.0001$; AEBSF, $P = 0.0004$; chymostatin; and CMK, $P = 0.0038$), five (GM6001), and seven (NEi) times; combined results are shown and compared using paired Student's *t* test. (B) Neutrophils were incubated with furin (100 ng/ml) or CMK 30 min before addition of R848. BAFF cell surface expression was analyzed by flow cytometry. The experiment was repeated seven times; combined results are shown and compared using paired Student's *t* test (R848, $P = 0.0095$; R848+Furin, $P = 0.0027$; R848+CMK, $P = 0.002$). (C) Neutrophils were incubated with furin (100 ng/ml) in presence or absence of R848 and analyzed for FcgRIIA levels by flow cytometry. The experiment was repeated nine times; combined results are shown. (D and E) Supernatant from activated neutrophils was fractionated and analyzed for capacity to induce shedding of monocyte FcgRIIA (D) without or (E) with prior boiling of the fractions. In E, the 30-kD pool was used. In panel D, the experiment was repeated four (30kD pool), six (10kD and 100 kD) or seven (30 kD fractions) times; combined results are shown and compared using paired Student's *t* test (>30 kD, $P = 0.0003$; <30 kD, $P = 0.0015$; 30 kD pool, $P = 0.016$ and $P = 0.018$ as compared with supernatant and <30 kD fraction, respectively; >10 kD, $P < 0.0001$; <10 kD, $P = 0.0002$; >100k D, $P = 0.0001$). In E, the experiment was repeated three (30 kD fraction and pool) or six (boiled supernatant) times; combined results are shown and compared using paired Student's *t* test (boiled supernatant, $P = 0.0035$; Boiled >30 kD, $P = 0.017$; Boiled <30 kD, $P = 0.011$). *, $P < 0.05$; **, $P < 0.01$; ***, $P < 0.001$.

TLR7/8-mediated shedding of FcgRIIA shifts neutrophil function from phagocytosis to NETosis

Given the ability of TLR7/8 to induce shedding of FcgRIIA, we asked what the biological consequences of FcgRIIA shedding on neutrophil key effector functions would be. As expected, after adding the furin inhibitor we observed a selective increase in the uptake of RNP-ICs, but not of latex beads (Fig. 5 A), consistent with a role for furin in promoting FcgRIIA shedding (Fig. 3 A). The furin inhibitor also amplified RNP-IC–mediated neutrophil activation (Fig. 5 B). However, in contrast to increased phagocytosis, addition of CMK decreased RNP-IC–mediated NETosis (Fig. 5 C). A similar phenomenon was observed using RNase treatment of RNP-ICs. Removal of the RNA component increased phagocytosis (Fig. 1 B) but reduced NETosis (Fig. 5 D), indicating opposite regulation of RNP-IC–mediated phagocytosis and NETosis in neutrophils. Importantly, RNase did not degrade the NETs (Fig. 5 E). RNase-mediated degradation of RNA in the SmRNP complex was also observed in the presence of anti-Sm/RNP autoantibodies (Fig. 5, F and G).

Because we observed contrasting effects with regard to TLR7/8 stimulation limiting phagocytosis while promoting NETosis, we asked if phagocytosis and NETosis were opposing processes in neutrophils. In support of this hypothesis, we found that addition of beads that stimulated phagocytosis

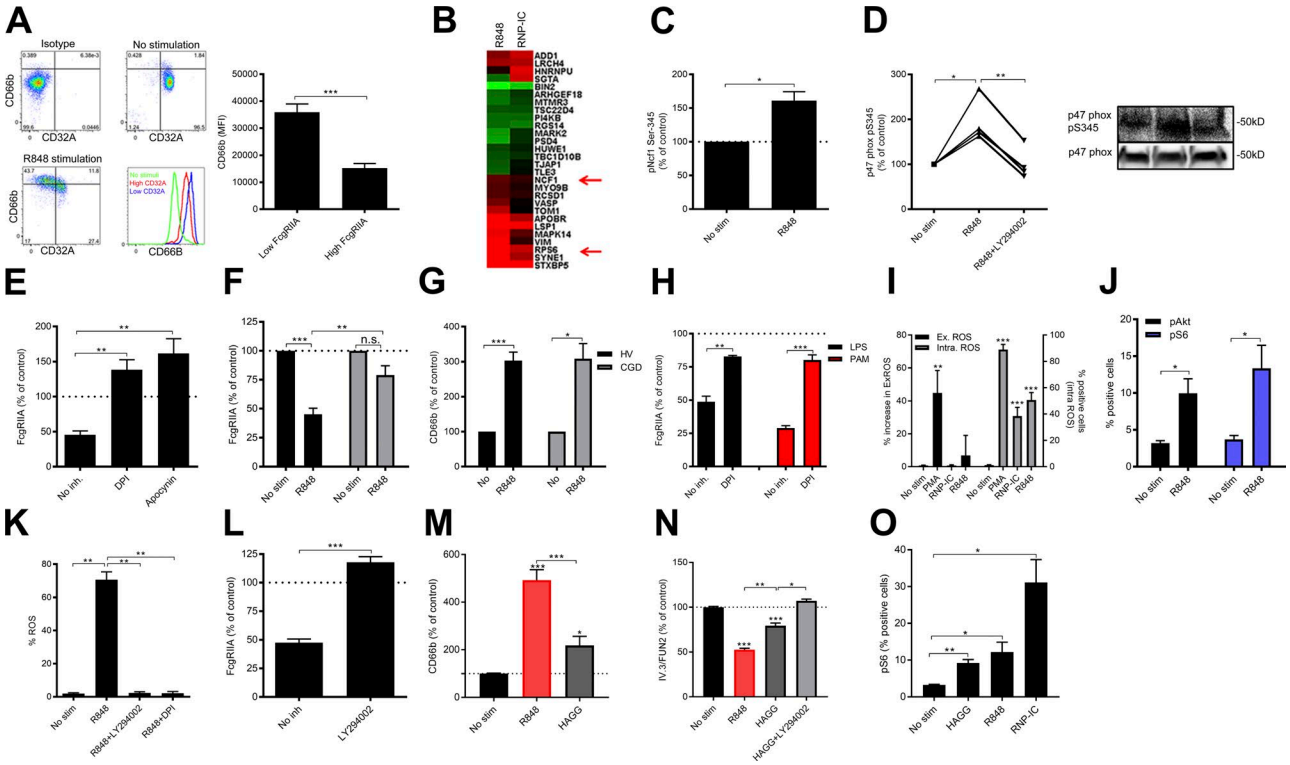

Figure 4. **FcgRIIA shedding requires reactive oxygen species.** (A) Neutrophils were activated with R848, and FcgRIIA and CD66b levels were analyzed by flow cytometry. The experiment was repeated eight times; combined results are shown and compared using paired Student's *t* test ($P < 0.0001$). (B) Heat-map illustrating phosphoproteins modified upon TLR7/8 activation by R848 and RNP-ICs. Results are expressed as fold change as compared with nonstimulated neutrophils with green representing decreased phosphorylation and red indicating increased phosphorylation. (C) Phosphorylated ncf1 (p47 phox) at S345 upon R848 activation as determined by phosphoproteomics. The experiment was repeated three times; combined results are shown and compared using paired Student's *t* test ($P = 0.044$). (D) Neutrophils were incubated with R848 in the absence or presence of the PI3K inhibitor Ly294002 and analyzed for pS345 or total levels of p47 phox using Western Blot. The experiment was repeated four times; combined results are shown and compared using paired *t* test (No stim, $P = 0.03$; R848+LY294002, $P = 0.0011$). (E) Neutrophils were treated with inhibitors of NADPH oxidase before addition of R848 and analyzed for cell surface expression of FcgRIIA by flow cytometry. The experiment was repeated six times; combined results are shown and compared using paired *t* test (DPI, $P = 0.0042$; Apocynin, $P = 0.0044$). (F) Neutrophils from healthy individuals (HV, $n = 18$) and CGD patients ($n = 4$) were stimulated with R848 and analyzed for FcgRIIA levels by flow cytometry. The data are analyzed using paired Student's *t* test (HC, $P < 0.0001$) and unpaired Student's *t* test (HC vs. CGD, $P = 0.0097$). (G) Neutrophils from healthy individuals (HV, $n = 13$) and CGD patients ($n = 3$) were activated by R848 and analyzed for CD66b expression by flow cytometry using paired Student's *t* test (HC, $P < 0.0001$; CGD, $P = 0.039$). (H) Neutrophils were activated with LPS or PAM3CSK4 in presence of DPI and analyzed for FcgRIIA levels by flow cytometry. The experiment was repeated four times; combined results are shown and compared using paired Student's *t* test (LPS, $P = 0.0062$; PAM, $P = 0.0003$). (I) Neutrophils were activated with R848, RNP-ICs, or PMA and analyzed for cellular localization for the ROS generation by flow cytometry and fluorimetry. The experiment was repeated five (extracellular) and eight (intracellular) times; combined results are shown and compared using paired Student's *t* test (Extracellular: PMA, $P = 0.007$; Intracellular: PMA, $P < 0.0001$; RNP-IC, $P = 0.0007$; R848, $P < 0.0001$). (J) Phosphorylation of Akt and S6 was determined by flow cytometry upon TLR7/8 activation. The experiment was repeated four times; combined results are shown and compared using paired *t* test (pS6, $P = 0.042$; pAkt, $P = 0.037$). (K) Neutrophils, pretreated with inhibitors of PI3K (LY294002, 10 µM) or NAD PH oxidase (DPI, 25 µM), were activated with R848 and analyzed for ROS generation by flow cytometry using DHR123. The experiment was repeated three times; combined results are shown and compared using paired Student's *t* test (R848, $P = 0.0049$; R848+LY294002, $P = 0.004$; R848+DPI, $P = 0.0031$). (L) Neutrophils were pretreated with the PI3K inhibitor LY294002 (10 µM) and analyzed for R848-mediated shedding of FcgRIIA by flow cytometry. The experiment was repeated eight times; combined results are shown and compared using paired Student's *t* test ($P < 0.0001$). (M–O) Neutrophils, with or without pretreatment with LY294002, were activated with heat-aggregated IgG (HAGG) and analyzed for (M) CD66b, (N) FcgRIIA shedding, and (O) pS6 expression by flow cytometry. In M and N, the experiments were repeated eight times. In O, the experiment was repeated five times; combined results are shown and compared using paired Student's *t* test (M: R848, $P < 0.0001$; HAGG, $P = 0.017$; R848 vs. HAGG, $P = 0.0001$; N: R848, $P < 0.0001$; HAGG, $P = 0.0002$; R848 vs. HAGG, $P = 0.0029$; HAGG vs. HAGG+LY294002, $P = 0.018$; O: HAGG, $P = 0.0024$; R848, $P = 0.0314$; RNP-IC, $P = 0.011$). *, $P < 0.05$; **, $P < 0.01$; ***, $P < 0.001$.

inhibited RNP-IC–mediated NETosis in a dose-dependent manner (Fig. 5 H). Addition of beads did not hinder subsequent uptake of RNP-ICs. On the contrary, neutrophils primed with phagocytic stimuli (beads) had an enhanced ability to phagocytose RNP-ICs, while losing the capacity to undergo NETosis (Fig. 5 I). Importantly, in neutrophils from healthy controls, high levels of full-length FcgRIIA were associated with an increased phagocytic ability, but de-

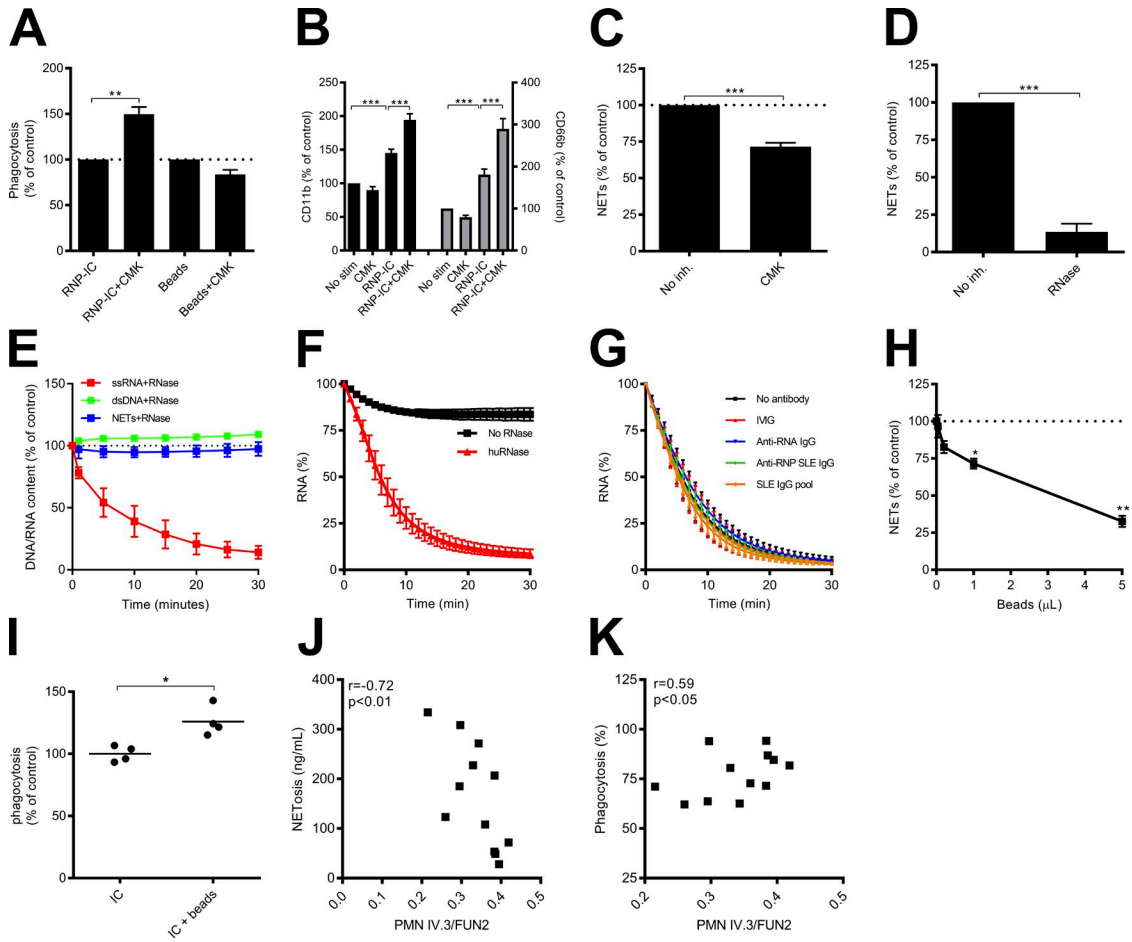

Figure 5. **FcgRIIA shedding differentially regulates neutrophil phagocytosis and NETosis.** (A) Neutrophils were incubated with CMK (25 µM), before addition of stimuli and phagocytosis analyzed by flow cytometry. The experiment was repeated five times; combined results are shown and compared using paired Student's *t* test (P = 0.0032). (B) Neutrophils were incubated with CMK before the addition of RNP-ICs and cell surface levels of CD11b and CD66b analyzed by flow cytometry. The results are expressed as CD11b or CD66b (percentage of control), as compared with nonstimulated cells. The experiment was repeated 15 times; combined results are compared using paired Student's *t* test (CD11b: RNP-IC; P < 0.0001; RNP-IC+CMK, P = 0.0002; CD66b: RNP-IC; P < 0.0001; RNP-IC+CMK, P < 0.0001). (C) Neutrophils, pretreated with CMK, were activated with RNP-ICs and the ability to release NETs analyzed by fluorimetry. The experiment was repeated six times; combined results are compared using paired Student's *t* test (P = 0.0001). (D) RNP-ICs were treated with RNases before addition to neutrophils and NET formation analyzed by fluorimetry. The experiment was repeated seven times; combined results are shown and compared using paired Student's *t* test (P < 0.0001). (E) SmRNP, NETs, dsDNA, or ssRNA were degraded by human RNase without (E and F) or with (G) presence of autoantibodies, and analyzed by fluorimetry over time. The experiment was repeated three (G), four (E), or eight (F) times. (H) NET formation was analyzed upon preincubation with different amounts of beads. The experiment was repeated three times; combined results are shown and compared using paired Student's *t* test (1 µl, P = 0.0135; 5 µl, P = 0.0031). (I) Neutrophil uptake of RNP-ICs was analyzed upon pretreatment with beads. The experiment was repeated four times; combined results are shown and compared using paired Student's *t* test (P = 0.018). (J and K) Neutrophils from healthy individuals (*n* = 12) were analyzed for baseline FcgRIIA IV.3/FUN2 ratio in relation to IC-mediated NETosis (J) and phagocytosis (K). The combined results are shown and analyzed using Spearman's correlation. *, P < 0.05; **, P < 0.01; ***, P < 0.001.

creased NET forming capacity of the neutrophils (Fig. 5, J and K), further verifying the inverse regulation between IC-mediated phagocytosis and NETosis. Thus, we have identified a novel process in which neutrophil function, through TLR7/8-mediated shedding of FcgRIIA, shifts from phagocytosis to NETosis. Importantly, the reverse also seems to be true, e.g., when neutrophils commit to phagocytosis they reduce their NET-inducing capacity.

Activation of neutrophil TLR7/8 results in proteolytic cleavage of FcgRIIA on monocytes and pDCs and a reduction in monocyte phagocytosis

Because we observed prominent protease-mediated shedding of FcgRIIA in neutrophils, we next asked if activated neutrophils could induce shedding of FcgRIIA in other immune cells. Although R848-induced monocyte activation and up-regulation of cell surface CD11b (unpublished data),

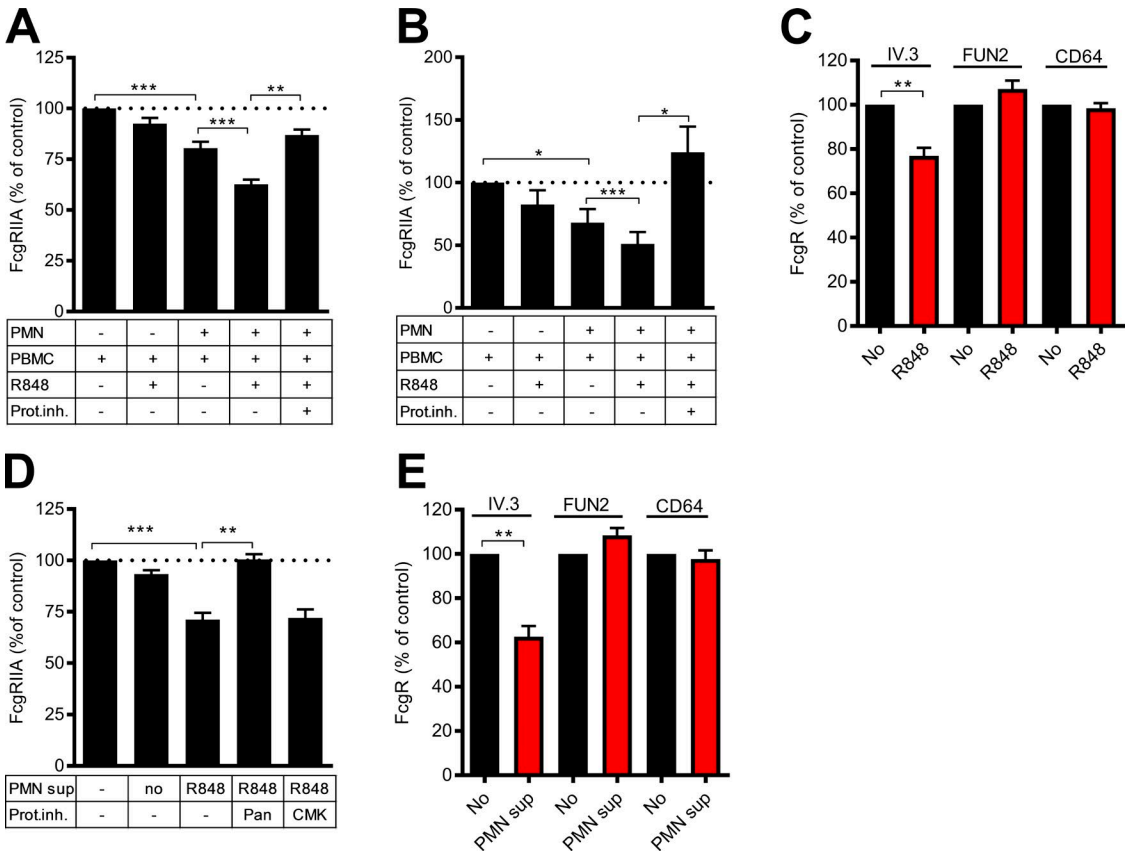

Figure 6. **TLR7/8-activated neutrophils shed FcgRIIA from monocytes and pDCs.** (A and B) PBMCs were coincubated with neutrophils (PMNs) in the presence of R848 and a pan-protease inhibitor. Levels of FcgRIIA on (A) monocytes ($CD14^+$) and (B) pDCs ($CD304^+$) were determined by flow cytometry and expressed as FcgRIIA (percentage of control) as compared with PBMCs incubated in medium in absence of neutrophils. In A, the experiment was repeated 11 times with the exception of the proteinase inhibitor ($n = 5$); combined results are shown and compared using paired *t* test (PMN+PBMC, $P < 0.0001$; PMN+PBMC vs. PMN+PBMC+R848, $P < 0.0001$; PMN+PBMC+R848 vs. PMN+PBMC+R848+Prot.inh., $P = 0.002$). In B, the experiment was repeated seven times; combined results are shown and compared using paired Student's *t* test (PMN+PBMC, $P = 0.0261$; PMN+PBMC vs. PMN+PBMC+R848, $P = 0.0002$; PMN+PBMC+R848 vs. PMN+PBMC+R848+Prot.inh., $P = 0.0128$). (C) Monocytes were analyzed for the expression of FcgRI (CD64), as well as FcgRIIA using the monoclonal antibodies IV.3 and FUN2. The experiment was repeated four times; combined results are shown and compared using paired Student's *t* test ($P = 0.008$). (D) Neutrophil supernatant, derived from nonstimulated (no, $n = 5$) or R848-stimulated (R848, $n = 9$) neutrophils, were added to monocytes in presence of indicated inhibitors (CMK; furin inhibitor, $n = 5$, and Pan; pan-protease inhibitor, $n = 5$) and monocyte FcgRIIA levels analyzed by flow cytometry. Combined results are shown and compared using paired Student's *t* test (R848, $P < 0.0001$; R848+Pan, $P = 0.003$). (E) Neutrophil supernatant were added to monocytes and expression of FcgRIIA (IV.3 and FUN2) as well as FcgRI (CD64) analyzed by flow cytometry. The experiment was repeated four times; combined results are shown and compared using paired Student's *t* test ($P = 0.0043$). *, $P < 0.05$; **, $P < 0.01$; ***, $P < 0.001$.

monocyte surface expression of FcgRIIA was unchanged (Fig. 6 A). However, upon co-culture with neutrophils primed with R848, monocytes lost cell surface FcgRIIA expression in a protease-dependent manner (Fig. 6 A). Similar findings were observed in pDCs, with loss of FcgRIIA in a neutrophil- and protease-dependent manner (Fig. 6 B). Comparable to what was observed in neutrophils, the loss of FcgRIIA expression on monocytes was selective for the IV.3 clone, as expression of neither the FUN2 epitope nor FcgRI was altered, indicating a similar protease was operative (Fig. 6 C). However, FUN-2 also targets FcgRIIB, even though it is expressed at much lower levels than FcgRIIA on monocytes (Su et al., 2007).

To determine if the loss of monocyte FcgRIIA was mediated through cell–cell interactions or through a soluble neutrophil-derived factor, we added supernatant from TLR7/8-activated neutrophils to monocytes. Cell-free supernatant from R848-activated neutrophils reduced monocyte FcgRIIA levels, indicating the presence of a soluble neutrophil factor able to mediate shedding of monocyte FcgRIIA (Fig. 6 D). The neutrophil supernatant shed monocyte FcgRIIA in a protease-dependent, but furin-independent manner, further demonstrating that furin does not act directly on FcgRIIA. Importantly, similar to what was observed in neutrophils stimulated directly or in the neutrophil-PBMC co-culture experiments, the supernatant derived from TLR-

7/8 activated neutrophils resulted in the selective shedding of the N-terminal region of the FcgRIIA (Fig. 6 E). Attempting to characterize the shed FcgRIIA by Western blot, recombinant FcgRIIA was incubated with neutrophil supernatant to cleave the receptor. Similar to what was found for the immune cells, addition of neutrophil supernatant led to a clear reduction in overall levels of full-length FcgRIIA. However, no low molecular fragment was observed either upon probing with clone IV.3 or using biotinylated FcgRIIA, suggesting that the degraded peptides were too small to be detected by Western blot (unpublished data). Although unlikely, considering the inability of R848 to induce shedding of FcgRIIA on monocytes and pDCs in PBMC cultures, an indirect role of another PBMC subset in mediating neutrophil-dependent shedding of monocyte and pDC FcgRIIA could not be ruled out.

As neutrophil proteases released after TLR activation promoted loss of FcgRIIA from monocytes and pDCs (Fig. 6, A and B), we next examined the functional consequences of shedding. Whereas monocyte phagocytosis of RNP-ICs was not affected by exposure to RNase or by priming with R848, the addition of neutrophil supernatant decreased monocyte phagocytosis of RNP-ICs by >50% (Fig. 7 A). To determine whether the reduction in IC phagocytosis impacted complement activation, we quantified release of the complement split product, C5a, by ELISA and observed that the reduced clearance of ICs induced increased generation of C5a (Fig. 7 B). This anaphylatoxin is known to promote inflammation and recruitment of immune cells, particular neutrophils (Guo and Ward, 2005). Consistent with this finding, SLE patients had increased C5a levels which correlated with shedding of neutrophil FcgRIIA (Fig. 7, C–E). Thus, we propose that neutrophil-mediated shedding of FcgRIIA on immune cells results in reduced FcgRIIA-mediated IC clearance in vivo. In normocomplementemic individuals, early complement components (C1q, C3) may provide a noninflammatory pathway for clearance (Elkon and Santer, 2012). However, in SLE patients who frequently have low levels of classical complement pathway components, activation and generation of C5a may lead to deleterious consequences (Elkon and Santer, 2012).

Selective FcgRIIA shedding is present in SLE patients and correlated with neutrophil activation

To investigate the potential clinical relevance of our observations, we analyzed cell surface levels of FcgRIIA on neutrophils and monocytes from patients with SLE, a disease where neutrophil abnormalities have been reported previously by us and others (Smith and Kaplan, 2015; Lood et al., 2016). Using the same two antibody clones to detect either full-length receptor (IV.3) or total levels (FUN2), we observed that neutrophils and monocytes from SLE patients demonstrated reduced expression of the most N-terminal portion of FcgRIIA as compared with healthy individuals (Fig. 8, A and B). Interestingly, low-density granulocytes (LDGs), known to spontaneously release NETs (Denny et al., 2010), had a greater degree of FcgRIIA shedding compared with their normal density counterparts (Fig. 8 C). SLE-derived neutrophils were overall activated and importantly, patients having high neutrophil activation had the lowest IV.3/FUN2 ratio (Fig. 8, D and E), consistent with our in vitro studies. Thus, ex vivo, neutrophil activation is associated with loss of FcgRIIA on neutrophils and monocytes.

As neutrophil and monocyte FcgRIIA shedding was highly correlated in SLE patients upon ex vivo analysis (Fig. 8 F), we asked whether this could be attributed to circulating proteases, likely neutrophil-derived. The addition of SLE serum, but not serum from healthy controls, induced shedding of FcgRIIA on neutrophils (Fig. 8 G), in a RNA- and protease-dependent manner (Fig. 8 H), suggesting that the presence of both RNA ICs and proteases participated in the shedding of FcgRIIA as was shown using purified components. Consistent with a role of RNA ICs, serum-mediated FcgRIIA shedding was higher in patients with anti-Sm/RNP antibodies (Fig. 8 I). To determine if serum-mediated shedding of FcgRIIA involved engulfment of RNP-ICs and subsequent de novo release of neutrophil proteases, healthy control neutrophils were incubated with a cytoskeletal inhibitor before addition of lupus sera. As illustrated in Fig. 8 H, addition of cytochalasin B almost completely abrogated serum-mediated FcgRIIA shedding, indicating that RNP-ICs needed to be internalized to promote shedding of FcgRIIA. Finally, SLE serum-mediated shedding of FcgRIIA from healthy control neutrophils strongly correlated with the FcgRIIA shedding observed upon ex vivo isolation of the SLE patient's neutrophils (Fig. 8 J). In summary, FcgRIIA on SLE monocytes and neutrophils demonstrate shedding at a site similar or identical to that identified by RNP-IC activated neutrophils in vitro, which can be attributed to RNA-ICs and proteases.

DISCUSSION

Previous studies have demonstrated an important role for IC-mediated induction of inflammation via neutrophils in the SLE pathogenesis (Garcia-Romo et al., 2011; Kaplan, 2011; Lood et al., 2016), but precisely how nucleoprotein-containing ICs impact recognition, phagocytosis, and subsequent induction of neutrophil effector functions have not been well characterized. In the current investigation, we made the novel finding that activation of TLR7/8, upon engulfment of RNP-ICs, induced proteolytic cleavage of FcgRIIA thereby shifting neutrophil function from phagocytosis of ICs to a program dedicated to NETosis. In contrast, when phagocytosis was increased by any one of three stimuli: blockade of TLR activation; inhibition of FcgRIIA shedding; or by priming neutrophils with a phagocytic stimulus, IC-mediated NETosis was markedly impaired. Together, these findings suggest an important cross regulation between phagocytosis and NETosis (Fig. 9). Our observations are consistent with the finding that phagocytosis of microbes led to a reduction in NETosis (Branzk et al., 2014). Thus, we propose that, in a process analogous to what has been described for DCs upon

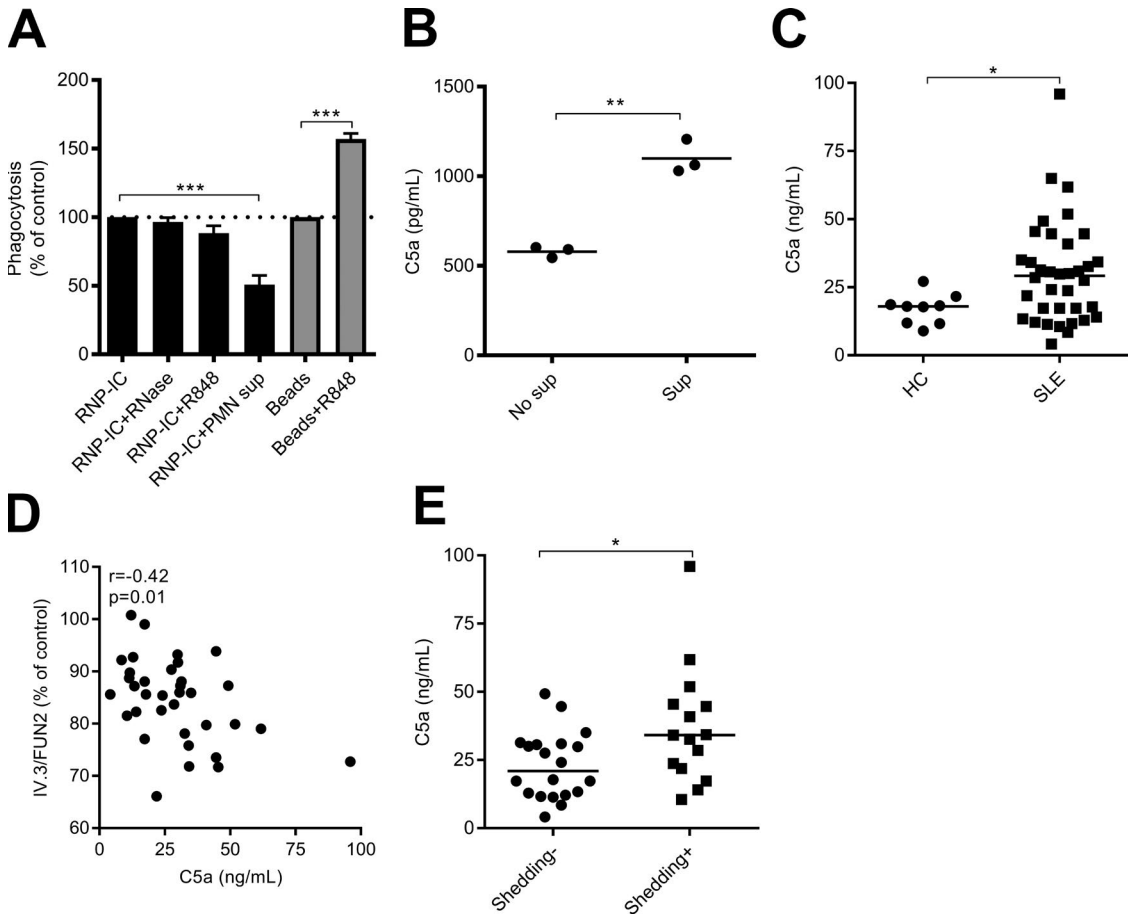

Figure 7. **Proteolytic cleavage of monocyte FcgRIIA inhibits clearance of ICs.** (A) Monocytes were incubated with R848 or neutrophil supernatant before addition of RNP-ICs or beads. Phagocytosis was determined by flow cytometry. The experiment was repeated four (beads, RNase, RNP-IC+R848) or seven (PMN sup) times; combined results are shown and compared using paired Student's *t* test (RNP-IC, P = 0.0003; Beads, P = 0.0007). (B) ICs were added to PBMCs with or without prior treatment with neutrophil supernatant (A). After phagocytosis for 30 min, remaining cell-free ICs were analyzed for C5a-inducing ability upon addition of 1% normal human serum. The experiment was repeated three times; combined results are shown and compared using paired *t* test (P = 0.0084). C) C5a serum levels were measured in healthy controls (HC, *n* = 9) and SLE patients (*n* = 36) by ELISA. Combined results are shown and analyzed using Mann-Whitney *U* test (P = 0.047). (D and E) Serum levels of C5a in SLE patients were related to ability of serum to induce shedding of FcgRIIA on healthy control neutrophils. In D, combined results from 35 SLE patients are shown and analyzed using Spearman's correlation test (r = −0.42; P = 0.011). In E, combined results are shown from SLE patients inducing shedding (*n* = 15) or not (*n* = 20), and compared using Mann-Whitney *U* test (P = 0.0281). *, P < 0.05; **, P < 0.01; ***, P < 0.001.

TLR activation, in which DCs lose their phagocytic capacity while gaining an effector function (antigen presentation) (Watts et al., 2010), TLR7/8 stimulation by RNP-ICs leads to a reduction in subsequent IC phagocytosis and dedicates neutrophils to a terminal effector function, NETosis. Interestingly, patients with SLE, known to have exuberant NET formation (Kaplan, 2011; Carmona-Rivera and Kaplan, 2014; Lood et al., 2016), as well as decreased phagocytic ability (Herrmann et al., 1998; Mevorach et al., 1998; Colonna et al., 2014), demonstrated substantial shedding of neutrophil FcgRIIA ex vivo, suggesting commitment of a proportion of their neutrophils toward the NET-inducing phenotype. Consistent with this interpretation, LDGs, that spontaneously generate NETs (Denny et al., 2010; Carmona-Rivera and Kaplan, 2013), had increased cleaved FcgRIIA as compared with their normal-density counterparts.

Loss of cell surface FcgRIIA has been described previously in human Langerhans cells (de la Salle et al., 1992) as well as neutrophils upon fMLP-mediated activation (Nagarajan et al., 2000), although the underlying mechanism(s) was not known. Following IC stimulation of neutrophils, we observed that only the most N-terminal portion of the FcgRIIA was shed as staining by the IV.3 antibody (that recognizes amino acids 132–137 of the second extracellular domain; Ramsland et al., 2011) was lost, yet recognition by FUN2 (epitope not known, Fig. 2 G), was retained. Enzyme inhibition studies implicated the pro-protein convertase, furin, as participating in the shedding of FcgRIIA, but this effect was not direct. Several

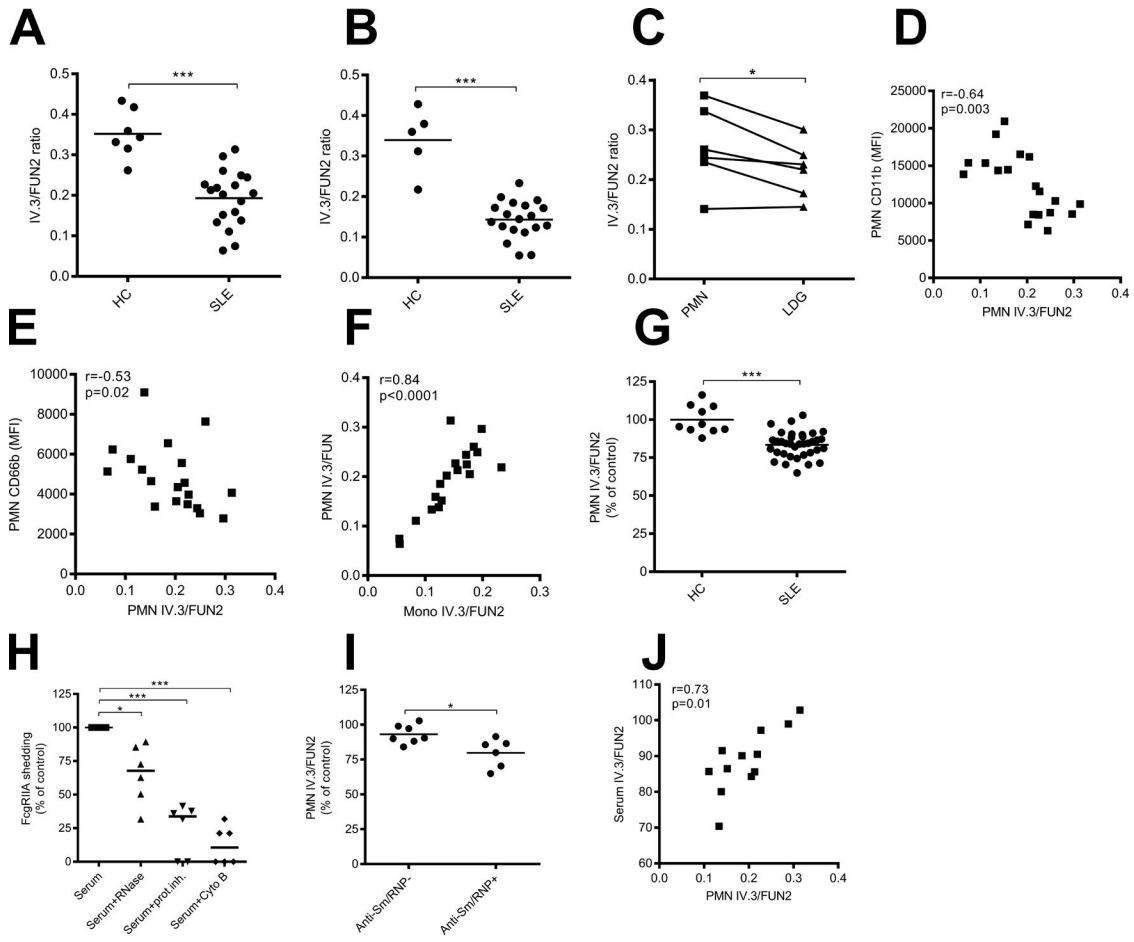

Figure 8. **SLE patients have increased FcgRIIA shedding related to neutrophil activation.** Neutrophils (A) and monocytes (B) were analyzed for FcgRIIA shedding using a ratio between shed FcgRIIA (IV.3) and total FcgRIIA levels (FUN2) in healthy controls (HC, n = 5–7) and SLE patients (n = 19). Combined results are shown and compared using Mann-Whitney U test (Neutrophils, P < 0.0001; Monocytes, P < 0.0001). (C) Normal-density neutrophils (PMNs) and low-density granulocytes (LDGs) were analyzed for FcgRIIA shedding by flow cytometry. Combined results from six SLE patients are shown and compared using paired Student's t test (P = 0.026). Neutrophil FcgRIIA shedding was correlated with neutrophil activation as measured by neutrophil CD11b (D) and CD66b expression (E) in SLE patients (n = 19). Combined results are analyzed using Spearman's correlation (CD66b, r = −0.64, P = 0.0029; CD11b, r = −0.53, P = 0.021). (F) Correlation analysis for ex vivo monocyte and neutrophil (PMN) FcgRIIA shedding in SLE patients. Combined results are analyzed using Spearman's correlation (r = 0.84; P < 0.0001). (G) Healthy control neutrophils were incubated with 10% serum from healthy controls (HC, n = 10) or SLE patients (n = 36) and analyzed for FcgRIIA shedding by flow cytometry as determined by the IV.3/FUN2 ratio. Combined results are shown and compared using Mann-Whitney U test (P < 0.0001). (H) Sera from 6 SLE patients, preincubated with either RNase, a pan-protease inhibitor (prot.inh.), or cytochalasin B (Cyto B; 5 µM) were added to neutrophils from a healthy individual and FcgRIIA shedding analyzed by flow cytometry. Combined results are shown and compared using paired Student's t test (RNase: P = 0.012; prot.inh.: P = 0.0002; Cyto B: P < 0.0001). (I) Serum-mediated shedding of FcgRIIA on healthy control neutrophils were analyzed in SLE patients with (n = 7) or without (n = 6) anti-Sm/RNP antibodies. Combined results are compared using Mann-Whitney U test (P = 0.035). (J) Correlation between ex vivo FcgRIIA shedding observed on SLE neutrophils with the shedding ability by the serum obtained from the same SLE patients (n = 12). Combined results are shown and analyzed by Spearman's correlation (r = 0.73; P = 0.0096). *, P < 0.05; **, P < 0.01; ***, P < 0.001.

other effects of furin may explain the action of this enzyme. There is a predicted furin cleavage site (Duckert et al., 2004) located at the junction of the transmembrane and intracytoplasmic domains so that intracellular furin cleavage could alter FcgRIIA conformation rendering it more susceptible to cleavage by another protease. Alternatively, or in addition, furin has been shown to be involved in the activation of several other proteases, including MMPs (Remacle et al., 2006) as well as ADAM10 and ADAM17 (Anders et al., 2001; Srour et al., 2003). ADAM17 has been implicated in shedding of FcgRII IB (Wang et al., 2013), but we were unable to inhibit FcgRIIA shedding by inhibitors of either MMPs or ADAM proteases. Furin may act even further upstream—furin-like proprotein convertases are essential in endosomal cleavage and subsequent activation of TLR7 and TLR8 (Hipp et al., 2013; Ishii et al., 2014). Although we did not observe an effect of furin inhibition on proteolytic activation of TLR8 in neutrophils, we observed that inhibition of furin reduced TLR7/8-mediated

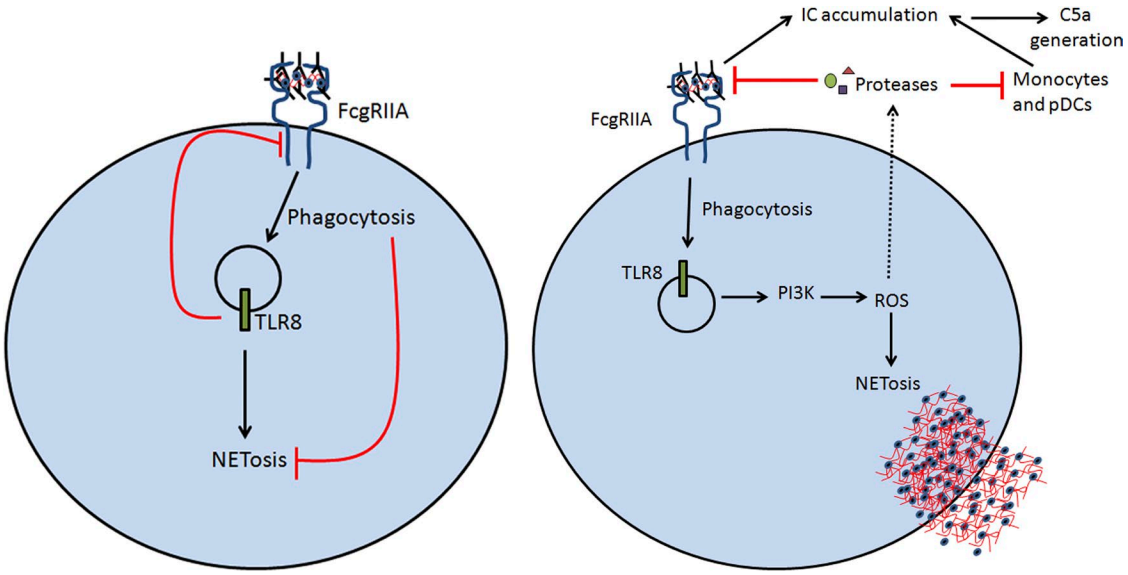

Figure 9. **Schematic overview of main findings.** Cartoons demonstrating the main findings described in the study. (left) Neutrophils may commit to phagocytosis or NETosis based on environmental triggers, in particular TLR activation. (right) Depiction of key signaling events resulting in TLR-mediated regulation of IC-mediated inflammation by neutrophils, monocytes, and pDCs. In brief, TLR activation results in activation of PI3K, contributing to generation of reactive oxygen species (ROS) via NADPH oxidase. ROS is essential for NET formation but also release of proteases able to shed FcgRIIA from immune cells. Loss of FcgRIIA results in increased ability of neutrophils to undergo IC-mediated NETosis, whereas also impairing phagocytic ability in neutrophils, monocytes, and pDCs. Noncleared ICs will instead activate the complement system to generate the anaphylatoxin C5a and be cleared through complement-dependent pathways.

ROS generation (unpublished data), which we showed here was necessary for FcgRIIa shedding. Further studies are needed to determine the furin substrates and which proteases other than furin are involved in the shedding of FcgRIIA.

Even though TLR7/8-mediated shedding of FcgRIIA was selective for neutrophils, transfer of neutrophil culture supernatant, or co-culture, enabled shedding of FcgRIIA on monocytes and pDCs, reducing their overall phagocytic ability. This resulted in increased generation of C5a, which promotes recruitment of neutrophils and macrophages, activation of phagocytic cells, release of granular proteins and generation of oxidants, all contributing to shaping the innate immunity and mediating tissue damage (Guo and Ward, 2005). Thus, we postulate that initial RNP-IC engagement of neutrophils promotes neutrophil maturation to NETosis as well as FcgRIIA shedding. By inducing shedding of FcgRIIA on adjacent immune cells, FcgRIIA-facilitated clearance of ICs as well as cytokine production are reduced whereas C5a facilitates recruitment of fresh phagocytes to remove ICs. In a normocomplementemic state, IC-bound C3b will facilitate resolution through clearance mechanisms that are less inflammatory (Lood et al., 2009; Santer et al., 2010; Colonna et al., 2014, 2016). However, in a hypocomplementemic state or with an abnormal CR3 (*ITGAM*) variants that impair clearance of IC by complement, as occurs in SLE (Harley et al., 2008; Nath et al., 2008; Fossati-Jimack et al., 2013), persistent activation of the terminal complement pathways will contribute to persistent inflammation.

Because shedding of FcgRIIA was not selective for TLR7/8, but observed for most of the TLR agonists tested, we asked what common signaling pathways could be involved in regulating FcgRIIA shedding. We found that shedding of FcgRIIA was mediated through the PI3K pathway and subsequent activation of NADPH oxidase as demonstrated by the use of selective inhibitors, as well as neutrophils obtained from CGD donors deficient in NADPH oxidase. Consistent with an impaired ability to undergo shedding of FcgRIIA in CGD patients, prior investigations have demonstrated an increased ability of CGD neutrophils to ingest ICs, although having similar baseline levels of FcgRIIA as healthy control neutrophils (Gaither et al., 1987). This is of particular interest as patients with impaired ROS production, thus unable to shed FcgRIIA and subsequently will promote phagocytosis by monocytes and pDCs, develop a type I IFN signature with a risk of autoimmunity, as observed in both SLE and CGD patients (Cunninghame Graham et al., 2011; Jacob et al., 2012; Kelkka et al., 2014; Lood et al., 2016). Although the role of ROS in this process is yet not fully understood, ROS has been shown to increase the sensitivity of target proteins for proteolytic degradation (Bota and Davies, 2002), and to activate redox-sensitive proteases (Scherz-Shouval et al., 2007). However, it should be acknowledged that ROS may act through several pathways to regulate inflammation and autoimmunity (Wen et al., 2016), including induction of hypoxia, which modulates the host response to inflammation, promoting resolution (Campbell et al., 2014).

In conclusion, we have identified an intricate cross talk between FcgRIIA and TLR7/8 that impacts phagocytosis and NETosis and unraveled several signal transduction pathways responsible. These observations extend our understanding of neutrophil function in regulation of autoimmunity and inflammation, and suggest that therapeutic interventions to prevent TLR7/8 activation would increase phagocytic clearance of ICs while limiting their ability to induce inflammatory NETosis.

MATERIAL AND METHODS

Patients and controls

All individuals signed informed consents in IRB-approved protocols (University of Washington, Seattle, WA; HSD number 39712). Pediatric samples from CGD individuals were obtained through the Seattle Children's Research Institute Center for Immunity and Immunotherapies Repository for Immune-Mediated Diseases.

NET induction and quantification

Human neutrophils were isolated by Polymorphprep (Axis-Shield) as described previously (Lood et al., 2016). Neutrophils (10^6 cells/ml) were incubated in poly-L-lysine–coated tissue culture plates with or without furin inhibitor chloromethylketone (CMK; 25 µM; Enzo Life Sciences), PI3K inhibitor LY294002 (10 µM; InvivoGen), pan-caspase inhibitor Q-VD-Oph (10 µM; Sigma-Aldrich), R848 (1 µg/ml; InvivoGen) or latex beads for 1 h before addition of PMA (20 nM), or RNP-ICs (IgG; purified from SLE patients with high titer anti-ribonucleoprotein [RNP] antibodies or healthy individuals, mixed with SmRNP [Arotec Diagnostic Limited], and used at final concentration of 10 µg/ml). In some experiments, RNP-ICs were pretreated with 0.25 mM human dimeric RNase-Fc for 30 min at 37°C before being used. NETs were detached with micrococcal nuclease (0.3 U/ml; Thermo Fisher Scientific) diluted in nuclease buffer containing 10 mM Tris-HCl, pH 7.5, 10 mM $MgCl_2$, 2 mM $CaCl_2$, and 50 mM NaCl. Detached NETs were quantified by analyzing Sytox Green (Life Technologies) intensity by plate reader (Synergy 2; BioTek).

Phagocytosis assay

SLE IgG, SmRNP, and heat-aggregated IgG (HAGG) were labeled with Alexa Fluor 647 according to manufacturer's protocol (Life Technologies). Neutrophils or PBMCs from healthy individuals were stimulated with different ICs, FITC-conjugated latex beads, or zymosan (100 µg/ml; Life Technologies) for 30 min at 37°C and immediately analyzed for phagocytosis. In blocking experiments, neutrophils were incubated with 0.1 µM TLR7-9 or control iODN (Enzo Life Sciences), CMK (25 µM; Enzo Life Sciences), cytochalasin B (5 µM; Sigma-Aldrich), or antibodies directed against CD16, CD32, or CD64 (all used at 10 µg/ml; BioLegend) for 30 min before addition of stimuli. In some experiments, R848, at a concentration of 2 µg/ml, or neutrophil supernatant, was added 30 and 90 min before addition of the phagocytic stimuli, respectively.

RNA degradation analysis

SmRNP, labeled with Sytox Green (8 µM), was incubated in the presence of huRNase (0.5 mM), IVIG, anti-RNA IgG, anti-RNP SLE IgG, or a pool of SLE IgG (all at 10 µg/ml) and analyzed for RNA degradation every minute for 30 min at 37°C using the Synergy 2 plate reader (BioTek). Results were normalized to the Sytox Green fluorescence level before addition of enzymes and expressed as percentage remaining RNA signal.

Neutrophil activation

Neutrophils were activated with LPS (1 µg/ml), R848 (2.5 µg/ml), PAM3CSK4 (5 µg/ml), CpG DNA (2 µg/ml; all from Invivogen), or RNP-ICs (10 µg/ml) for 4 h, with or without prior addition of CMK (25 µM; Enzo Life Sciences) for 60 min. Activation was analyzed by flow cytometry (FacsCanto; BD) by assessing cell surface levels of CD66b and CD11b (BioLegend). Data were analyzed by FlowJo (Tree Star, Inc.).

FcgRIIA shedding: flow cytometry

Neutrophils were activated by LPS (1 µg/ml), R848 (2 µg/ml), PAM3CSK4 (5 µg/ml), Loxoribine (0.1 mM), CL075 (2.5 µg/ml), or CpG DNA (2 µg/ml) for 30 min, followed by analysis of cell surface expression of CD32A (IV.3; StemCell Technologies; FUN-2; BioLegend), CD16 (clone 3G8), CD64 (clone 10.1), and CD66b (all from BioLegend) by flow cytometry. For intracellular staining, neutrophils were fixed in 2% paraformaldehyde for 10 min, permeabilized with saponin (diluted 1:1000 in PBS) for 15 min, and stained with anti-CD32A antibodies diluted 1:100. In some experiments, neutrophils were incubated with inhibitors (DPI (25 µM; Sigma-Aldrich), apocynin (100 µM; Sigma-Aldrich), GM-6001 (10 µM; Enzo Life Sciences), LY294002 (10 µM), cOmplete Protease Inhibitor Cocktail Tablets (1X dissolved in H_2O; Roche), neutrophil elastase IV inhibitor (25 µM; EMD Millipore), E-64 (1 µM; Sigma-Aldrich), 4-(2-Aminoethyl) benzenesulfonyl fluoride hydrochloride (AEBSF; 0.1 mM; Sigma-Aldrich), CMK (25 µM, Enzo Life Sciences), cytochalasin B (5 µM, Sigma-Aldrich), or chymostatin (10 µg/ml; Sigma-Aldrich), or recombinant furin (100 ng/ml; maximal dose tolerated by the neutrophils; PeproTech) 30 min before addition of stimuli. In some experiments, cell surface levels of B cell–activating factor (BAFF; BioLegend) was analyzed according to the same protocol as described above. Monocytes and pDCs were detected using antibodies to CD14 (BioLegend) and CD304 (Miltenyi Biotec), respectively.

FcgRIIA shedding: fluorimetry

For detection of shed FcgRIIA, neutrophils were prelabeled with FITC-conjugated anti-CD32A antibody IV.3 (StemCell Technologies) or FITC-conjugated anti-CD32A antibody FUN-2 (BioLegend), and washed extensively before

activation with R848. Cell-free supernatant was analyzed for shed FcgRIIA–anti-CD32A-FITC complexes by fluorimetry (Synergy 2; BioTek) using anti-CD32A antibodies as a standard curve. In some experiments, cells were preincubated with the pan protease inhibitor cocktail (Roche).

FcgRIIA shedding: Western blot

Recombinant FcgRIIA (Novoprotein), biotinylated (Thermo Fisher Scientific) or nonbiotinylated, was incubated with neutrophil supernatant for 2 h and analyzed for cleavage fragments using Western blot, probing with streptavidin-HRP, or antibody clone IV.3, respectively.

Mass spectrometry and bioinformatics

Neutrophils, 4×10^6 cells distributed in eight tubes, were treated with medium (baseline), RNP-ICs, or R848 (5 μg/ml) for 15 min at 37°C. Pelleted cells were lysed with 6 M urea in 50 mM NH_4HCO_3 (Thermo Fisher Scientific) supplemented with Halt Phosphatase Inhibitor Cocktail (Thermo Fisher Scientific). Cell debris was removed by centrifugation (20,000 *g* for 15 min). For reduction and denaturation of the peptides, the samples were incubated with TCEP (37°C; 5 mM; Thermo Fisher Scientific), iodoacetamine (30 mM final concentration; Bio-Rad Laboratories), and DTT (30 mM final concentration; Bio-Rad Laboratories) for 1 h each. Samples were aliquoted at 100 and 800 μl 25 mM NH_4HCO_3, and 200 μl MeOH (Thermo Fisher Scientific) was added to each tube, followed by trypsin digestion (Promega; 1:50 wt/wt) for 16 h at 37°C. Trypsinated samples were washed three times in H_2O, followed by speedvac, and resuspended in 200 μl acetonitrile (ACN) with 0.1% trifluoroacetic acid (TFA; Thermo Fisher Scientific). Samples were desalted with MacroSpin Columns (The Nest Group), saturated with 80% ACN in 0.1% TFA, and equilibrated with 5% ACN in 0.1% TFA. The samples were run through the columns twice, and desalted samples were eluted with 80% ACN in 0.1% TFA. Phosphopeptides were isolated using the TiO_2 Phosphopeptide Enrichment and Clean-up kit according to the manufacturer's instructions (Thermo Fisher Scientific). In brief, samples were added to phosphopeptide-binding TiO_2 spin tips, followed by removal of nonphosphopeptides by wash steps. Eluted phosphopeptides were cleaned in graphite columns and eluted in 50% ACN in 0.1% formic acid, followed by speedvac, and adjustment of samples to 0.1% formic acid in 5% ACN. Isolated phosphoproteins were analyzed by OrbiTrap Fusion Tribrid Mass spectrometer (Thermo Fisher Scientific). Data were extracted using MaxQuant software. Samples were normalized through dividing with the total phosphorylation level in each sample, followed by $\log_2$ transformation. KEGG analysis was done using DAVID, and the heat map using Gene Cluster 3.0 and Java Treeview.

p47 phox Western blot

Neutrophils (5×10^6 cells in 250 μl) were incubated with inhibitor of PI3K (LY294002, 10 μM) or pan protease inhibitor cocktail (1×) 30 min before addition of stimuli, and incubated for an additional 60 min. Neutrophil cell lysates were run on an SDS-PAGE. For the Western blot, antibodies to phosphorylated S345 (Assay Biotech) or total p47-phow (Thermo Fisher Scientific) were added at 1/1000, and detected using anti–rabbit IgG-HRP (GE Healthcare; 1/5,000) followed by Super Signal West Pico Chemiluminescent Substrate (Thermo Fisher Scientific) according to manufacturer's recommendations.

ROS analysis

Neutrophils were incubated with inhibitors (LY294002 [10 μM], CMK [25 μM], DPI [25 μM], or pan protease inhibitor cocktail [1×]) for 30 min before addition of R848 (2 μg/ml) for an additional 60 min. DHR123 (30 μM; Sigma-Aldrich), was added during the last 30 min of incubation, and ROS analyzed by flow cytometry. For determination of extracellular ROS production upon neutrophil activation, OxyBURST Green H2HFF BSA (25 μg/ml) was used according to the manufacturer's instructions (Thermo Fisher Scientific).

Analysis of S6 and Akt phosphorylation by flow cytometry

Neutrophils were activated by R848 for 15 min, fixed, and permeabilized according to manufacturer's instructions (BioLegend), and incubated with a specific antibody recognizing phosphorylated S235/236 in S6 (Cell Signaling Technology) or phosphorylated S473 in Akt (BD) for 60 min. pS6 and pAkt levels were analyzed by flow cytometry and expressed as percent positive cells as compared with nonstimulated cells.

Incubation of PBMCs with neutrophils or neutrophil supernatant

Neutrophils and PBMCs were incubated at a 2:1 ratio (500,000 vs. 250,000 cells) with the pan-protease inhibitor (1×) for 30 min followed by R848 (2 μg/ml) for an additional 60 min and analyzed for FcgR levels by flow cytometry. Plasmacytoid DCs were identified based on their expression of BDCA-4 (Miltenyi Biotec) and monocytes based on their expression of CD14 (BioLegend). In some experiments neutrophil supernatant (generated by incubating neutrophils with R848 for 90 min) were added to PBMCs with or without presence of the pan-protease inhibitor (1X), and expression of FcgRs and phagocytic ability analyzed in monocytes by flow cytometry as described in the Phagocytosis assay and FcgRIIA shedding: flow cytometry section.

C5a generation

PBMCs were incubated with or without neutrophil supernatant for 90 min as described above, and allowed to engulf RNP-ICs for 30 min. Cell-free ICs were isolated and incubated with 1% normal human serum for 3 h at 37°C. C5a generation, as well as C5a levels in serum from healthy controls and SLE patients, was analyzed by ELISA according to the manufacturer's instructions (R&D Systems).

Statistics

For group comparisons, student's two-tailed unpaired or paired *t* test was used. For the comparison between SLE patients and healthy controls the Mann-Whitney *U* test was used. Spearman's correlation test was used for all correlation analyses. Data are presented as bar graphs with mean and SEM, or dot plots with medians. All analyses were considered statistically significant at $P < 0.05$.

ACKNOWLEDGMENTS

We would like to thank Edward Clark and Eric Butz for valuable discussions, Jie An, Xizhang Sun, and Sudeshna Seal for technical assistance; Anne Stevens and Troy Torgerson for CGD patient samples; and Laura Durcan and Judy Juo for characterization of the SLE patients.

The study was supported by grants from the Leap for Lupus Foundation (K.B. Elkon), the Wenner-Gren Foundation (C. Lood), and the foundation BLANCEFLOR Boncompagni-Ludovisi née Bildt (C. Lood).

K.B. Elkon and J. Ledbetter are inventors of a human RNase-Fc protein (Resolve Therapeutics). The authors declare no additional conflicts of interest.

Author contributions: C. Lood participated in the conceptualization of the idea, designed and performed experiments, analyzed the results, supervised S. Arve, and drafted the manuscript. S. Arve performed experiments and analyzed results. J. Ledbetter participated in the conceptualization of the idea and designed experiments. K.B. Elkon participated in the conceptualization of the idea, designed experiments, and drafted the manuscript. All authors critically revised the manuscript and approved the final version.

Submitted: 9 September 2016

Revised: 21 November 2016

Accepted: 19 April 2017

REFERENCES

Anders, A., S. Gilbert, W. Garten, R. Postina, and F. Fahrenholz. 2001. Regulation of the alpha-secretase ADAM10 by its prodomain and proprotein convertases. *FASEB J.* 15:1837–1839.

Assi, L.K., S.H. Wong, A. Ludwig, K. Raza, C. Gordon, M. Salmon, J.M. Lord, and D. Scheel-Toellner. 2007. Tumor necrosis factor alpha activates release of B lymphocyte stimulator by neutrophils infiltrating the rheumatoid joint. *Arthritis Rheum.* 56:1776–1786. http://dx.doi.org/10.1002/art.22697

Berger, M., C.Y. Hsieh, M. Bakele, V. Marcos, N. Rieber, M. Kormann, L. Mays, L. Hofer, O. Neth, L.Vitkov, et al. 2012. Neutrophils express distinct RNA receptors in a non-canonical way. *J. Biol. Chem.* 287:19409–19417. http://dx.doi.org/10.1074/jbc.M112.353557

Blander, J.M., and R. Medzhitov. 2004. Regulation of phagosome maturation by signals from toll-like receptors. *Science.* 304:1014–1018. http://dx.doi.org/10.1126/science.1096158

Bota, D.A., and K.J. Davies. 2002. Lon protease preferentially degrades oxidized mitochondrial aconitase by an ATP-stimulated mechanism. *Nat. Cell Biol.* 4:674–680. http://dx.doi.org/10.1038/ncb836

Branzk, N., A. Lubojemska, S.E. Hardison, Q. Wang, M.G. Gutierrez, G.D. Brown, and V. Papayannopoulos. 2014. Neutrophils sense microbe size and selectively release neutrophil extracellular traps in response to large pathogens. *Nat. Immunol.* 15:1017–1025. http://dx.doi.org/10.1038/ni.2987

Campbell, E.L., W.J. Bruyninckx, C.J. Kelly, L.E. Glover, E.N. McNamee, B.E. Bowers, A.J. Bayless, M. Scully, B.J. Saeedi, L. Golden-Mason, et al. 2014. Transmigrating neutrophils shape the mucosal microenvironment through localized oxygen depletion to influence resolution of inflammation. *Immunity.* 40:66–77. http://dx.doi.org/10.1016/j.immuni.2013.11.020

Carmona-Rivera, C., and M.J. Kaplan. 2013. Low-density granulocytes: a distinct class of neutrophils in systemic autoimmunity. *Semin. Immunopathol.* 35:455–463. http://dx.doi.org/10.1007/s00281-013-0375-7

Carmona-Rivera, C., and M.J. Kaplan. 2014. Detection of SLE antigens in neutrophil extracellular traps (NETs). *Methods Mol. Biol.* 1134:151–161. http://dx.doi.org/10.1007/978-1-4939-0326-9_11

Chen, K., H. Nishi, R. Travers, N. Tsuboi, K. Martinod, D.D. Wagner, R. Stan, K. Croce, and T.N. Mayadas. 2012. Endocytosis of soluble immune complexes leads to their clearance by FcγRIIIB but induces neutrophil extracellular traps via FcγRIIA in vivo. *Blood.* 120:4421–4431. http://dx.doi.org/10.1182/blood-2011-12-401133

Colonna, L., C. Lood, and K.B. Elkon. 2014. Beyond apoptosis in lupus. *Curr. Opin. Rheumatol.* 26:459–466. http://dx.doi.org/10.1097/BOR.0000000000000083

Colonna, L., G.C. Parry, S. Panicker, and K.B. Elkon. 2016. Uncoupling complement C1s activation from C1q binding in apoptotic cell phagocytosis and immunosuppressive capacity. *Clin. Immunol.* 163:84–90. http://dx.doi.org/10.1016/j.clim.2015.12.017

Cunninghame Graham, D.S., D.L. Morris, T.R. Bhangale, L.A. Criswell, A.C. Syvänen, L. Rönnblom, T.W. Behrens, R.R. Graham, and T.J.Vyse. 2011. Association of NCF2, IKZF1, IRF8, IFIH1, and TYK2 with systemic lupus erythematosus. *PLoS Genet.* 7:e1002341. http://dx.doi.org/10.1371/journal.pgen.1002341

Dang, P.M., A. Stensballe, T. Boussetta, H. Raad, C. Dewas, Y. Kroviarski, G. Hayem, O.N. Jensen, M.A. Gougerot-Pocidalo, and J. El-Benna. 2006. A specific p47phox-serine phosphorylated by convergent MAPKs mediates neutrophil NADPH oxidase priming at inflammatory sites. *J. Clin. Invest.* 116:2033–2043. http://dx.doi.org/10.1172/JCI27544

de la Salle, C., M.E. Esposito-Farese, T. Bieber, J. Moncuit, M. Morales, A. Wollenberg, H. de la Salle, W.H. Fridman, J.P. Cazenave, J.L. Teillaud, et al. 1992. Release of soluble Fc gamma RII/CD32 molecules by human Langerhans cells: a subtle balance between shedding and secretion? *J. Invest. Dermatol.* 99:15S–17S. http://dx.doi.org/10.1111/1523-1747.ep12668250

Denny, M.F., S.Yalavarthi, W. Zhao, S.G.Thacker, M.Anderson, A.R. Sandy, W.J. McCune, and M.J. Kaplan. 2010. A distinct subset of proinflammatory neutrophils isolated from patients with systemic lupus erythematosus induces vascular damage and synthesizes type I IFNs. *J. Immunol.* 184:3284–3297. http://dx.doi.org/10.4049/jimmunol.0902199

Doyle, S.E., R.M. O'Connell, G.A. Miranda, S.A. Vaidya, E.K. Chow, P.T. Liu, S. Suzuki, N. Suzuki, R.L. Modlin, W.C. Yeh, et al. 2004. Toll-like receptors induce a phagocytic gene program through p38. *J. Exp. Med.* 199:81–90. http://dx.doi.org/10.1084/jem.20031237

Duckert, P., S. Brunak, and N. Blom. 2004. Prediction of proprotein convertase cleavage sites. *Protein Eng. Des. Sel.* 17:107–112. http://dx.doi.org/10.1093/protein/gzh013

Elkon, K.B., and D.M. Santer. 2012. Complement, interferon and lupus. *Curr. Opin. Immunol.* 24:665–670. http://dx.doi.org/10.1016/j.coi.2012.08.004

Eloranta, M.L., G.V. Alm, and L. Rönnblom. 2013. Disease mechanisms in rheumatology--tools and pathways: plasmacytoid dendritic cells and their role in autoimmune rheumatic diseases. *Arthritis Rheum.* 65:853–863. http://dx.doi.org/10.1002/art.37821

Fossati-Jimack, L., G.S. Ling, A. Cortini, M. Szajna, T.H. Malik, J.U. McDonald, M.C. Pickering, H.T. Cook, P.R. Taylor, and M. Botto. 2013. Phagocytosis is the main CR3-mediated function affected by the lupus-associated variant of CD11b in human myeloid cells. *PLoS One.* 8:e57082. http://dx.doi.org/10.1371/journal.pone.0057082

Gaither, T.A., S.R. Medley, J.I. Gallin, and M.M. Frank. 1987. Studies of phagocytosis in chronic granulomatous disease. *Inflammation.* 11:211–227. http://dx.doi.org/10.1007/BF00916022

Garcia-Romo, G.S., S. Caielli, B. Vega, J. Connolly, F. Allantaz, Z. Xu, M. Punaro, J. Baisch, C. Guiducci, R.L. Coffman, et al. 2011. Netting

neutrophils are major inducers of type I IFN production in pediatric systemic lupus erythematosus. *Sci. Transl. Med.* 3:73ra20. http://dx.doi.org/10.1126/scitranslmed.3001201

Gullstrand, B., M.H. Lefort, H. Tydén, A. Jönsen, C. Lood, A. Johansson, S. Jacobsen, L. Truedsson, and A.A. Bengtsson. 2012. Combination of autoantibodies against different histone proteins influences complement-dependent phagocytosis of necrotic cell material by polymorphonuclear leukocytes in systemic lupus erythematosus. *J. Rheumatol.* 39:1619–1627. http://dx.doi.org/10.3899/jrheum.111511

Guo, R.F., and P.A. Ward. 2005. Role of C5a in inflammatory responses. *Annu. Rev. Immunol.* 23:821–852. http://dx.doi.org/10.1146/annurev.immunol.23.021704.115835

Hargraves, M.M., H. Richmond, and R. Morton. 1948. Presentation of two bone marrow elements; the tart cell and the L.E. cell. *Proc. Staff Meet. Mayo Clin.* 23:25–28.

Harley, J.B., M.E. Alarcón-Riquelme, L.A. Criswell, C.O. Jacob, R.P. Kimberly, K.L. Moser, B.P. Tsao, T.J. Vyse, C.D. Langefeld, S.K. Nath, et al. International Consortium for Systemic Lupus Erythematosus Genetics (SLEGEN). 2008. Genome-wide association scan in women with systemic lupus erythematosus identifies susceptibility variants in ITG AM, PXK, KIAA1542 and other loci. *Nat. Genet.* 40:204–210. http://dx.doi.org/10.1038/ng.81

Hawkins, P.T., K. Davidson, and L.R. Stephens. 2007. The role of PI3Ks in the regulation of the neutrophil NADPH oxidase. *Biochem. Soc. Symp.* 74:59–67. http://dx.doi.org/10.1042/BSS2007c06

Hayashi, F., T.K. Means, and A.D. Luster. 2003. Toll-like receptors stimulate human neutrophil function. *Blood.* 102:2660–2669. http://dx.doi.org/10.1182/blood-2003-04-1078

Herrmann, M., R.E. Voll, O.M. Zoller, M. Hagenhofer, B.B. Ponner, and J.R. Kalden. 1998. Impaired phagocytosis of apoptotic cell material by monocyte-derived macrophages from patients with systemic lupus erythematosus. *Arthritis Rheum.* 41:1241–1250. http://dx.doi.org/10.1002/1529-0131(199807)41:7<1241::AID-ART15>3.0.CO;2-H

Hipp, M.M., D. Shepherd, U. Gileadi, M.C. Aichinger, B.M. Kessler, M.J. Edelmann, R. Essalmani, N.G. Seidah, C. Reis e Sousa, and V. Cerundolo. 2013. Processing of human toll-like receptor 7 by furin-like proprotein convertases is required for its accumulation and activity in endosomes. *Immunity.* 39:711–721. http://dx.doi.org/10.1016/j.immuni.2013.09.004

Ishii, N., K. Funami, M. Tatematsu, T. Seya, and M. Matsumoto. 2014. Endosomal localization of TLR8 confers distinctive proteolytic processing on human myeloid cells. *J. Immunol.* 193:5118–5128. http://dx.doi.org/10.4049/jimmunol.1401375

Jacob, C.O., M. Eisenstein, M.C. Dinauer, W. Ming, Q. Liu, S. John, F.P. Quismorio Jr., A. Reiff, B.L. Myones, K.M. Kaufman, et al. 2012. Lupus-associated causal mutation in neutrophil cytosolic factor 2 (NCF2) brings unique insights to the structure and function of NADPH oxidase. *Proc. Natl. Acad. Sci. USA.* 109:E59–E67. http://dx.doi.org/10.1073/pnas.1113251108

Kaplan, M.J. 2011. Neutrophils in the pathogenesis and manifestations of SLE. *Nat. Rev. Rheumatol.* 7:691–699. http://dx.doi.org/10.1038/nrrheum.2011.132

Kaplan, M.J., and M. Radic. 2012. Neutrophil extracellular traps: double-edged swords of innate immunity. *J. Immunol.* 189:2689–2695. http://dx.doi.org/10.4049/jimmunol.1201719

Kelkka, T., D. Kienhöfer, M. Hoffmann, M. Linja, K. Wing, O. Sareila, M. Hultqvist, E. Laajala, Z. Chen, J. Vasconcelos, et al. 2014. Reactive oxygen species deficiency induces autoimmunity with type 1 interferon signature. *Antioxid. Redox Signal.* 21:2231–2245. http://dx.doi.org/10.1089/ars.2013.5828

Kolaczkowska, E., and P. Kubes. 2013. Neutrophil recruitment and function in health and inflammation. *Nat. Rev. Immunol.* 13:159–175. http://dx.doi.org/10.1038/nri3399

Kulkarni, S., C. Sitaru, Z. Jakus, K.E. Anderson, G. Damoulakis, K. Davidson, M. Hirose, J. Juss, D. Oxley, T.A. Chessa, et al. 2011. PI3Kβ plays a critical role in neutrophil activation by immune complexes. *Sci. Signal.* 4:ra23. http://dx.doi.org/10.1126/scisignal.2001617

Lood, C., and G.C. Hughes. 2016. Neutrophil extracellular traps as a potential source of autoantigen in cocaine-associated autoimmunity. *Rheumatology.* 56:638–643.

Lood, C., B. Gullstrand, L. Truedsson, A.I. Olin, G.V. Alm, L. Rönnblom, G. Sturfelt, M.L. Eloranta, and A.A. Bengtsson. 2009. C1q inhibits immune complex-induced interferon-alpha production in plasmacytoid dendritic cells: a novel link between C1q deficiency and systemic lupus erythematosus pathogenesis. *Arthritis Rheum.* 60:3081–3090. http://dx.doi.org/10.1002/art.24852

Lood, C., L.P. Blanco, M.M. Purmalek, C. Carmona-Rivera, S.S. De Ravin, C.K. Smith, H.L. Malech, J.A. Ledbetter, K.B. Elkon, and M.J. Kaplan. 2016. Neutrophil extracellular traps enriched in oxidized mitochondrial DNA are interferogenic and contribute to lupus-like disease. *Nat. Med.* 22:146–153. http://dx.doi.org/10.1038/nm.4027

Mevorach, D., J.O. Mascarenhas, D. Gershov, and K.B. Elkon. 1998. Complement-dependent clearance of apoptotic cells by human macrophages. *J. Exp. Med.* 188:2313–2320. http://dx.doi.org/10.1084/jem.188.12.2313

Nagarajan, S., K. Venkiteswaran, M. Anderson, U. Sayed, C. Zhu, and P. Selvaraj. 2000. Cell-specific, activation-dependent regulation of neutrophil CD32A ligand-binding function. *Blood.* 95:1069–1077.

Nath, S.K., S. Han, X. Kim-Howard, J.A. Kelly, P. Viswanathan, G.S. Gilkeson, W. Chen, C. Zhu, R.P. McEver, R.P. Kimberly, et al. 2008. A nonsynonymous functional variant in integrin-alpha(M) (encoded by ITGAM) is associated with systemic lupus erythematosus. *Nat. Genet.* 40:152–154. http://dx.doi.org/10.1038/ng.71

Nathan, C. 2006. Neutrophils and immunity: challenges and opportunities. *Nat. Rev. Immunol.* 6:173–182. http://dx.doi.org/10.1038/nri1785

Pham, C.T. 2006. Neutrophil serine proteases: specific regulators of inflammation. *Nat. Rev. Immunol.* 6:541–550. http://dx.doi.org/10.1038/nri1841

Ramsland, P.A., W. Farrugia, T.M. Bradford, C.T. Sardjono, S. Esparon, H.M. Trist, M.S. Powell, P.S. Tan, A.C. Cendron, B.D. Wines, et al. 2011. Structural basis for Fc gammaRIIa recognition of human IgG and formation of inflammatory signaling complexes. *J. Immunol.* 187:3208–3217. http://dx.doi.org/10.4049/jimmunol.1101467

Remacle, A.G., D.V. Rozanov, M. Fugere, R. Day, and A.Y. Strongin. 2006. Furin regulates the intracellular activation and the uptake rate of cell surface-associated MT1-MMP. *Oncogene.* 25:5648–5655. http://dx.doi.org/10.1038/sj.onc.1209572

Santer, D.M., B.E. Hall, T.C. George, S. Tangsombatvisit, C.L. Liu, P.D. Arkwright, and K.B. Elkon. 2010. C1q deficiency leads to the defective suppression of IFN-alpha in response to nucleoprotein containing immune complexes. *J. Immunol.* 185:4738–4749. http://dx.doi.org/10.4049/jimmunol.1001731

Scherz-Shouval, R., E. Shvets, E. Fass, H. Shorer, L. Gil, and Z. Elazar. 2007. Reactive oxygen species are essential for autophagy and specifically regulate the activity of Atg4. *EMBO J.* 26:1749–1760. http://dx.doi.org/10.1038/sj.emboj.7601623

Smith, C.K., and M.J. Kaplan. 2015. The role of neutrophils in the pathogenesis of systemic lupus erythematosus. *Curr. Opin. Rheumatol.* 27:448–453. http://dx.doi.org/10.1097/BOR.0000000000000197

Srour, N., A. Lebel, S. McMahon, I. Fournier, M. Fugère, R. Day, and C.M. Dubois. 2003. TACE/ADAM-17 maturation and activation of sheddase activity require proprotein convertase activity. *FEBS Lett.* 554:275–283. http://dx.doi.org/10.1016/S0014-5793(03)01159-1

Su, K., H. Yang, X. Li, X. Li, A.W. Gibson, J.M. Cafardi, T. Zhou, J.C. Edberg, and R.P. Kimberly. 2007. Expression profile of FcgammaRIIb on leukocytes and its dysregulation in systemic lupus erythematosus. *J.*

Immunol. 178:3272–3280. http://dx.doi.org/10.4049/jimmunol.178.5.3272

Villanueva, E., S. Yalavarthi, C.C. Berthier, J.B. Hodgin, R. Khandpur, A.M. Lin, C.J. Rubin, W. Zhao, S.H. Olsen, M. Klinker, et al. 2011. Netting neutrophils induce endothelial damage, infiltrate tissues, and expose immunostimulatory molecules in systemic lupus erythematosus. *J. Immunol.* 187:538–552. http://dx.doi.org/10.4049/jimmunol.1100450

Wang, Y., J. Wu, R. Newton, N.S. Bahaie, C. Long, and B. Walcheck. 2013. ADAM17 cleaves CD16b (FcγRIIIb) in human neutrophils. *Biochim. Biophys. Acta.* 1833:680–685. http://dx.doi.org/10.1016/j.bbamcr.2012.11.027

Watts, C., M.A. West, and R. Zaru. 2010. TLR signalling regulated antigen presentation in dendritic cells. *Curr. Opin. Immunol.* 22:124–130. http://dx.doi.org/10.1016/j.coi.2009.12.005

Wen, Z., Y. Shimojima, T. Shirai, Y. Li, J. Ju, Z. Yang, L. Tian, J.J. Goronzy, and C.M. Weyand. 2016. NADPH oxidase deficiency underlies dysfunction of aged $CD8^+$ Tregs. *J. Clin. Invest.* 126:1953–1967. http://dx.doi.org/10.1172/JCI84181